Effects of extreme climatic events on the hydrological parameters of the estuarine waters of the Amazon Coast

Ádila Kelly Rodrigues da Costa[1], Luci Cajueiro Carneiro Pereira[2,a] , José A. Jiménez[3] , Antonio Rafael Gomes de Oliveira[4], Manuel de Jesus Flores-Montes[5] and Rauquírio Marinho da Costa[6]

[1]Universidade Federal do Pará, Instituto de Estudos Costeiros, Laboratório de Oceanografia Costeira e Estuarina, Alameda Leandro Ribeiro sn, Aldeia, 68600-000, Braganca-Pará. E-mail: adila.rc@hotmail.com

[2]Universidade Federal do Pará, Instituto de Estudos Costeiros, Laboratório de Oceanografia Costeira e Estuarina, Alameda Leandro Ribeiro sn, Aldeia, 68600-000, Braganca-Pará. E-mail: cajueiro@ufpa.br.

[3]Universitat Politècnica de Catalunya - BarcelonaTech, Laboratori d'Enginyeria Marítima, C/Jordi Girona, 1-3, 08034, Barcelona, Spain. E-mail: jose.jimenez@upc.edu.

[4]Universidade Federal do Pará, Instituto de Estudos Costeiros, Laboratório de Plâncton e Cultivo de Microalgas, Alameda Leandro Ribeiro sn, Aldeia, 68600-000, Braganca-Pará. E-mail: faelolive02@gmail.com

[5]Universidade Federal de Pernambuco, Departamento de Oceanografia, Avenida Arquitetura, s/n, Cidade Universitária, Recife, Pernambuco. E-mail: manuel@ufpe.br.

[6]Universidade Federal do Pará, Instituto de Estudos Costeiros, Laboratório de Plâncton e Cultivo de Microalgas, Alameda Leandro Ribeiro sn, Aldeia, 68600-000, Braganca-Pará. E-mail: raucosta@ufpa.br.

[a] Corresponding Author. Luci Cajueiro Carneiro Pereira. E-mail: cajueiro@ufpa.br. Phone:+559134251209.

Acknowledgements

This study was financed by Conselho Nacional de Desenvolvimento Científico e Tecnológico (CNPq), through a Universal project (483913/2012-0), and by CAPES (Ciências do Mar II - 88882.158649/2014-01). The authors Pereira LCC (309491/2018-5) and Costa RM (311782/2017-5) would also like to thank CNPq for research grants, and Costa AK and is grateful to Coordenação de Aperfeiçoamento de Pessoal de Nível Superior (CAPES) for research grants. We are also indebted to Stephen Ferrari for his careful revision of the English.

Abstract

Oscillations in rainfall levels are one of the principal factors that determine seasonal shifts in physicochemical and hydrobiological variables, and exceptional climate events can have an enormous effect on the characteristics of small tropical estuaries. Given this, the present study investigated the responses of the physiochemical and hydrobiological variables of a small, shallow and well-mixed Amazonian estuary with absence of any direct fluvial discharge to different climatic scenarios (typical conditions, and drier events). The study was based on 21 field campaigns conducted between April 2012 and April 2017. During rainy seasons of typical condition, when rainfall levels were higher and salinity lower than 7 (just after a weak La Niña), phytoplankton biomass was affected by increased turbidity (> 400 NTU) of the water, even when nitrogenous compounds were readily available (ammonium: 3.39 ± 1.71 µmol L^{-1}, nitrite 0.90 ± 0.80 µmol L^{-1} and nitrate (3.91 ± 1.86 µmol L^{-1}). In addition, the absence of any direct fluvial discharge appear has contributed to the cumulation of phytoplankton biomass (chlorophyll-a > 20 mg m^{-3}) into the estuary during the rainy season of the drier events and typical condition, when turbidity was lower (< 200 NTU). Conversely, during the dry seasons of the drier events, when rainfall levels were lower, and extremes of salinity were recorded (>38), phytoplankton biomass (chlorophyll-a < 10 mg m^{-3}) was affected by the lower levels of nitrogenous compounds, even when phosphorous compounds were largely available. Overall, the present study has shown that extreme oscillations in rainfall levels cause abrupt shifts in the physicochemical parameters of the estuary, and affected the phytoplankton biomass, although high turbidity appeared to limit the buildup of this biomass. These effects are manifested immediately in the study area, given that the Taperaçu is a small estuary with a limited freshwater input, and it would seem reasonable to expect similar processes in other minor Amazonian estuaries when subjected to extreme fluctuations in rainfall levels.

Key words: Climatic events, hydrological variables, estuary, Amazon coast.

1. Introduction

Estuaries are often associated with mangroves in equatorial and tropical regions. Estuarine mangrove environments are among the world's most productive ecosystems, with high rates of primary production, and substantial autotrophic and heterotrophic biomass (Bianchi 2007; Burford et al. 2008; Arumugam et al. 2016). These areas are characterized by a well-defined climatic cycle, typically with two main seasons, rainy and dry (Geyer et al. 1996). This cycle controls the freshwater input into the system, and determines the functional mechanisms of the estuarine ecosystem (Santos et al. 2008; Goes et al. 2014). However, these areas may be affected by extreme fluctuations in climatic conditions, driven primarily by large-scale climate oscillations such as the El Niño Southern Oscillation-ENSO (Gomez et al. 2019; Francisco and Neto 2020).

The ENSO includes both positive (El Niño) and negative (La Niña) anomalies in the temperature of the surface waters of the equatorial Pacific Ocean (Grimm et al. 1998). During El Niño events, the surface waters of the tropical Pacific are warmer than normal, which may decrease rainfall in the Amazon region and, as a consequence, reduce the volume of fluvial discharge (Restrepo et al. 2014). The most intense El Niño events in the past few decades were the result of the exceptional warming of the surface temperature of the eastern Pacific, combined with a major redistribution of global atmospheric humidity and temperature (Xue and Kumar 2016; Barnard et al. 2017). These processes caused severe droughts in Australia, India, and Central America (Chiew et al. 1998; Changnon 1999), Africa (Eltahir 1996), Indonesia (Siegert and Marsiat 2001), Peru (Marengo et al. 2012), and Amazonia (Marengo et al. 2008, 2016). During La Niña events, by contrast, a major decrease in the temperature of the surface waters of the tropical Pacific in the vicinity of northern Australia, New Guinea, and Indonesia (Feng et al. 2013; Palutikof et al. 2015)

causes rainier-than-normal conditions over these areas, as well as in southeastern Africa (Moeletsi et al. 2011; Zaroug et al. 2014) and northern Brazil (Marengo et al. 2011).

These climatic fluctuations affect estuaries by modifying one of the principal hydrodynamic forces, i.e. the input of freshwater, which in turn may modify saline stratification patterns, seawater intrusion, renewal time, and the processes inherent to the biogeochemical cycles (Grimm et al. 2000; Garcia et al. 2004). During drier conditions, estuarine waters become more saline, and dissolved inorganic nutrient concentrations decline (Wilkerson et al. 2002; Wetz et al. 2011; Valiela et al. 2013), with the opposite pattern being observed during events of increased rainfall (Valiela et al. 2012; Thompson et al. 2015). These alterations affect biological productivity, and impact fishery production, which may have serious socio-economic implications (Garcia et al. 2004; Rossi and Soares 2017).

Located in the equatorial zone, the Amazon coast is highly susceptible to the effects of these climatic oscillations. This region includes the world's largest continuous tract of mangrove forest, which is influenced by the discharge of the Amazon River and dozens of other local estuaries (Kjerfve and Lacerda 1993; Goes et al. 2014). This complex system of estuaries releases one of the greatest inputs of dissolved nutrients and organic matter to the ocean (DeMaster and Pope 1996; Geyer et al. 1996). In recent years, the estuaries of the Amazon coast have been subjected by both La Niña and El Niño events (Pereira et al. 2013; Andrade et al. 2016), in addition to a major drought, provoked by an anomalous northward migration of the Atlantic Intertropical Convergence Zone (ITCZ), as a consequence of the increase in the temperature of the surface waters of the tropical Atlantic Ocean (Marengo et al. 2012, 2013a, 2013b; Pereira et al. 2017; Cunha et al. 2019).

Previous studies on the Amazon coast found that the temporal variation in hydrological factors is influenced primarily by oscillations in rainfall levels (Pereira et al. 2012; Pamplona et al. 2013). However, the effects on estuarine environments of the fluctuations in the physical, chemical, and biological variables related to those extreme climatic events have not been documented systematically. It is thus necessary to expand the available database on the Amazon coast to better understand and predict the response of these variables under different, in particular extreme conditions. As the Taperaçu is a small estuary with less than 30 km in length, relatively small changes in forcing conditions may result in immediate impacts in the functioning of the estuary due to the extension of the domain affected. This means that estuaries of small size are appropriate for the modeling of the functioning of these systems under varying conditions (Callaway et al. 2014; Andrade et al. 2016) and the Taperaçu can be considered to be a paradigm of this type of estuarine environment. In this context, the hypothesis of the present study is that the phytoplankton biomass will scale to the level of rainfall to a certain point, after which the effects of light limitation will prevent biomass buildup. We believe that these effects are more intense during the rainy season, given that the dry season accounts for less than 15% of the annual rainfall.

To test this hypothesis, we evaluated the patterns of variation in biotic and abiotic data (such as temperature, salinity, pH, turbidity, nutrient concentrations, and phytoplankton biomass) during periods influenced by different climatic events, that is, low rainfall (El Niño and drought) and typical condition (including a post weak La Niña) in the Taperaçu estuary, on the Amazon coast. It is hoped that the determination of the degree of association between the variation in estuarine dynamics and extreme fluctuations in

71 climatic patterns can be used to model and predict the variation in similar systems located
72 in equatorial and tropical regions around the world.
73
74 **2. Material and Methods**
75 2.1 Study Area
76 The present study focused on the Taperaçu estuary in eastern Brazilian Amazonia.
77 Taperaçu estuary is typical for the northern coast of Brazil. This estuary is located on the
78 Bragança Peninsula (in the municipality of Bragança), approximately 150 km southeast of
79 the mouth of the Amazon River (Figure 1). This peninsula is covered by a well-developed
80 mangrove forest, which covers a total area of more than 180 km^2 (Krause et al. 2001), and
81 is dominated by three mangrove tree species, *Rhizophora mangle* L., *Avicennia germinans*
82 L., and *Laguncularia racemosa* (L.) C.F. Gaertn (Cohen et al. 1999; Menezes et al. 2008).
83
84 <Insert Figure 1>
85
86 The Taperaçu is a small, funnel-shaped estuary, with a basin of 40 km^2, of which,
87 21 km^2 is covered with water surface (Araújo Jr. and Asp 2013). With less than 30 km in
88 length, the mean depth of this estuary is 4 m, and extensive sandbanks run longitudinally
89 along its mid-sector. Freshwater input is relatively small, with the main sources being the
90 Taicí channel (Fig. 1), which connects the Taperaçu to the neighboring Caeté estuary (Asp
91 et al. 2012), and the Tamatateua channel, which transports freshwater from the adjacent
92 marshes, that are inundated during the rainy season. The local semi-diurnal tides may reach
93 heights of 5–6 m near the mouth of the Taperaçu estuary during the spring tide. Tidal
94 currents are typical of a shallow estuary, reaching velocities of over 1.5 m s^{-1} (Asp et al.

2012). Waves play only a secondary role in the hydrodynamics of estuary, with their propagation being mediated by the sandbanks (Asp et al. 2013).

The local climate is hot and humid equatorial, with a relatively intense rainy season, typically between January and June (Martorano et al. 1993). The rainiest months are between March and May, when more than 80% of the annual rainfall is usually recorded (INMET 2019). The driest months are between September and November, when rainfall is negligible, resulting in an excess of evaporation (INMET 2019). Wind directions and speeds also vary seasonally, with relatively strong northeasterly winds (mean monthly speeds of 2.8-4.4 m s^{-1}, with a maximum of 6.9-9.3 m s^{-1}) during the dry season. Winds are much weaker during the rainy season, coming from all the directions, with mean monthly speeds of 1.4-3.1 m s^{-1}, increasing to a maximum of 4.1-7.1 m s^{-1} (Pereira et al. 2012; INMET 2019).

The historical mean annual rainfall (1982–2017) of the study area is 2,360 mm, and data series indicates that 85% of the annual rainfall occurs during the rainy season months, with this pattern being modified during extreme climatic events (Online Resource 1).

2.2 Sample collection and laboratory methods

Hourly rainfall levels were obtained for the period between April 2012 and April 2017 from the Brazilian National Meteorological Institute's (INMET) Tracuateua station, that is located to 36 m above the ground, and approximately 33 km northeast of the mouth of the Taperaçu estuary. Physicochemical (water temperature, salinity, turbidity, pH, ammonium, nitrite, nitrate, dissolved organic nitrogen - DON, total dissolved nitrogen - TDN, orthophosphate, dissolved organic phosphorous - DOP, total dissolved phosphorous - TDP and silicate concentrations) and biological (chlorophyll-a concentrations) data were

collected during 21 campaigns (Online Resource 2) at three sampling stations in the lower, middle, and upper sectors of the estuary (Fig. 1). Each of the campaigns lasted 25 hours and were conducted under different climatic periods, including: (i) an intense drought (2012 and 2013), which was characterized by a deficit in the annual rainfall of 34% in 2012 and 32% in 2013; (ii) a typical rainfall period (2014 and part of the first half of 2015) with mean values similar to historical data; (iii) a strong El Niño event (between the second half of 2015 and November 2016), when a 25% rainfall deficit was recorded, and (iv) another typical year, which occurred just after a weak La Niña event. This La Niña event began at the end of 2016, but weakened in the middle of the first half of 2017. The events were classified based on Cunha et al. (2019) and government websites (INMET 2019; Golden Gate Weather Service 2021), as shown in Online Resource 2.

A bottom-mounted mooring was installed at each station, to which the CTDs (conductivity, temperature and depth) were attached. Readings were taken every 10 min over the 25-h sample period (total = 150 readings) by each CTD (RBRmaestro) equipped with turbidity sensors. For temperature, the CTD was accurate to ±0.002°C, while for conductivity, it was accurate to ±0.0003 S m^{-1}. The profiles derived from the processed data were exported using the Ruskin software for further analysis.

Niskin bottles were cast every 3 hours to obtain water samples at a depth of 1 m below the surface. A total of 567 water samples were collected during this study. These samples were preserved in a cooler at 4ºC for transportation to the laboratory, where the pH, and dissolved nutrient and chlorophyll-a concentrations were immediately determined.

In the laboratory, the pH of the water samples was measured using a tabletop pH-meter (HANNA HI 2221), with resolution of 0.01. Water samples were vacuum-filtered through glass-fiber filters (Whatman GF/F 0.7 μm, 47 mm), and both the samples and the

filters were freeze-dried for further analyses of nutrients and chlorophyll-a, respectively. The chlorophyll-a (Chl-a) was extracted with 90% acetone *v/v* and determined spectrophotometrically, following the Parsons and Strickland (1963) and UNESCO (1966) protocols. The concentrations of dissolved organic nutrients (nitrite - NO_2^-, nitrate - NO_3^-, ammonium - NH_4^+, orthophosphate - PO_4^{3-} and silicate - DSi) were also determined by spectrophotometry, using the procedures described by Strickland and Parsons (1972) and Grasshoff et al. (1983). The total dissolved nitrogen and total dissolved phosphorus were determined by applying an adaptation of the simultaneous oxidation of the nitrogen and phosphorus compounds using an alkaline persulfate-oxidizing solution (Grasshoff et al. 1999).

A Thermo Scientific 220 Evolution UV-Vis spectrophotometer was used to analyze the nutrient and chlorophyll-a concentrations. This spectrophotometer was calibrated with deionized water (mixed bed deionizer Q-380M), and the detection limits (DL) established for the analyses were: nitrate (DL = 0.05 μmol L^{-1}), nitrite (DL = 0.01 μmol L^{-1}), ammonium (DL = 0.05 μmol L^{-1}), silicate (DL = 0.1 μmol L^{-1}), orthophosphate (DL = 0.03 μmol L^{-1}), and chlorophyll-a (DL = 0.02 mg m^{-3}). To guarantee quality control, the linearity of the chemical method (R^2>0.998) was determined using individual calibration curves compiled using standard solutions of known concentrations of the respective substances.

2.3 Statistical analysis

The temporal variation in the physiochemical and hydrobiological data was analyzed by month, season, and climatic condition (typical period, and drought and El Niño events) between April, 2012, and April, 2017. Spearman correlation coefficients were used

166 to examine the influence of rainfall levels on the variables analyzed. The Lilliefors test
167 (Conover 1971) was applied to verify the normality of the abiotic (water temperature,
168 salinity, pH, turbidity, and nutrient concentrations) and biotic data (chlorophyll-a). When
169 the data were not normal or homogeneous, they were *log* (x + 1) transformed to produce a
170 near-normal or near-homogeneous distribution.

171 A one-way Analysis of Variance (ANOVA) was then used to evaluate the variation
172 in the data at different time scales ((monthly, seasonal and seasonal per climatic events).
173 The parameters that varied in this analysis were tested to determine the specific effects of
174 the different climatic periods. When the data were not homogeneous, the nonparametric
175 Mann-Whitney *U* or Kruskal-Wallis *H* tests were applied to determine the variation in the
176 data (Zar 1999). When a significant difference was found among seasons or events, *a*
177 *posteriori* pairwise comparisons were applied, based on the Fisher LSD test and the
178 Student-Newman-Keuls analysis. A two-way ANOVA was used to examine the interaction
179 (seasonal *vs* events) among physiochemical and hydrobiological variables.

180 Principal Component Analysis (PCA) was employed to determine the relationships
181 between environmental variables (temperature, salinity, turbidity, pH, chlorophyll-a,
182 ammonium, nitrite, nitrate, DON, TDN, orthophosphate, DOP, TDP and silicate) using the
183 CANOCO 4.5 software (Ter Braak and Smilauer 2002). For this analysis, correlation
184 matrices (Legendre and Legendre 2012) were used in order to identify seasonal patterns
185 under the influence of the effects of typical, drought and El Niño conditions. The data were
186 ordered in relation to the respective variables, from the covariance matrices, which were
187 transformed and/or standardized according to their amplitude of variation (Milligan and
188 Cooper 1988; Legendre and Legendre 2012).

189

3. Results

The influence of rainfall levels on the hydrological variables is clearly indicated through the Spearman correlation. In table 1, the Spearman coefficients showed positive correlations between rainfall and the following variables: turbidity (r_s = 0.282, p < 0.001), ammonium (r_s = 0.121; p = 0.004), nitrite (r_s = 0.379; p < 0.001), nitrate (r_s = 0.170; p < 0.001), TDN (r_s = 0.107; p = 0.011) and chlorophyll-a (r_s = 0.111; p = 0.008). Spearman coefficients analysis also revealed a negative correlation between rainfall and salinity (r_s = −0.840; p < 0.001). Rainfall was also correlated negatively with pH (r_s = −0.138; p = 0.001), orthophosphate (r_s = −0.439; p < 0.001), DOP (r_s = −0.158; p < 0.001), TDP (r_s = −0.401; p < 0.001) and silicate (r_s = −0.103; p = 0.014).

PCA also confirmed that the environmental variables contributed to explain the seasonal distribution between the samples analyzed (Figure 2). The first two axes of PCA ordering explained 37.1% of the total variance associated with the environment-rainfall relationship. The first axis highlighted the differences between the rainy (square symbols) and dry (circles) symbols season samples, while on the second axis it was revealed a notable separation of the dry period (Figs. 2a, b). On the first axis, the rainy season has been associated with the high concentrations of ammonium, nitrite, nitrate, turbidity, DON and TDN (Fig. 2a, c). Conversely, a negative association has been related to high values of salinity, during the dry period, as well as with ortophosphate concentrations, TDP, DOP and temperature, mainly during the drought and the El Niño events (Fig. 2b). In the second axis, the concentrations of silicate, chlorophyll-a and turbidity were associated with the high rainfall observed in the rainy season of the drought, typical and *El Niño* conditions, and negatively associated with low pH, which was associated with the dry season.

Figure 3a presents the deficit of cumulative 3 months of rainfall data (%), which shows clearly the 16–31% deficit in rainfall levels recorded during the drier events when compared with the mean rainfall data. Given the observed dependence of most variables with rainfall, the relationship among the physiochemical variables and phytoplankton biomass (chlorophyll-a) was analyzed under different climatic conditions (see Figures 3–5, Table 2).

The beginning of this study is marked by a strong drought that occurred between January 2012 and December 2013, when rainfall levels – 1552 mm in 2012 and 1612 mm in 2013 – were well below average (Fig. 3a). Eight campaigns were conducted during this period, in April, June, September, and December, 2012, and March, June, September, and December, 2013. During this drought event, differences were recorded among months in all the study variables (Table 2). Salinity – for example – reached mean values of 38% above normal. Thus, lower rainfall levels recorded during this event were responsible for the highest values of salinity (38.7 ± 0.4, December 2013, Fig. 3c), phosphorus compounds (orthophosphate: 1.65 ± 0.82 µmol L^{-1}, Fig. 5a; TDP: 1.8± 0.84 µmol L^{-1}, Fig. 5c; both in December 2012), and chlorophyll-a (29.6 ± 9.0 mg m^{-3}, April 2012, Fig. 5e) recorded at any time during the six years of the study period. At the opposite extreme, this period was also responsible for the lowest values of nitrite (0.01 ± 0.1 µmol L^{-1}, December 2012, Fig. 4b), nitrate (1.07 ± 1.26 µmol L^{-1}, April 2012, Fig. 4c), DON (0.30 ± 0.43 µmol L^{-1}, December 2013, Fig. 4d) and silicate (18.9 ± 12.2 µmol L^{-1}, April 2012, Fig. 5d) recorded during the six years of the study period.

The months between January 2014 and April 2015 can be considered to be a typical period in terms of rainfall (Fig. 3a). Five campaigns were conducted during this period in April, June, September and December, 2014, and March, 2015. In this study period, as

237 expected, salinity (Fig. 3c) was lower during the rainy season months, with the lowest
238 values being recorded in April 2014 (6.9 ± 0.8), and the highest, during the dry season
239 (38.2 ± 3.4, December 2014), when evaporation exceeded rainfall. The pH of the water was
240 slightly alkaline (Fig. 3d) and varied in a similar pattern to that of salinity, with the lowest
241 values being recorded in the rainy season (April 2014, 7.3 ± 0.3) and the highest in the dry
242 season (December 2014, 7.9 ± 0.5). The water was least turbid (Fig. 3e) in December 2014
243 (80.1 ± 72.7 NTU) and most turbid in March 2015 (355.3 ± 337.8 NTU).

244 The highest concentrations of the nitrogenous compounds (Fig. 4a-e) were recorded
245 during the rainy season, reaching 3.10 ± 2.02 µmol L^{-1} for ammonium in April 2014, 3.10 ±
246 2.84 µmol L^{-1} for nitrate (in March 2015), 0.17 ± 0.12 µmol L^{-1} for nitrite (March 2015),
247 4.61 ± 2.83 µmol L^{-1} for DON (in April 2014) and 9.46 ± 1.96 µmol L^{-1} for TDN in April
248 2014. By contrast, the highest concentrations of phosphorus compounds (orthophosphate:
249 1.16 ± 0.66 µmol L^{-1} and TDP: 1.60 ± 0.39 µmol L^{-1}, Figs. 5a, c) and DSi (86.5 ± 54.1
250 µmol L^{-1}, Fig. 5d) were recorded during the dry season (December 2014). The highest
251 mean chlorophyll-a concentrations were recorded in April 2014 (27.2 ± 19.5 mg m^{-3}, Fig.
252 5e) and the lowest in March 2015 (7.75 ± 6.96 mg m^{-3}).
253
254 <Insert Figure 2>
255 <Insert Figure 3>
256 <Insert Figure 4>
257 <Insert Figure 5>
258
259 After this typical period, a strong El Niño event occurred during the study period,
260 lasting 19 months. Seven campaigns were conducted during this period, in June,

September, and December, 2015, and in April, June, September, and November, 2016. With the exception of silicate (H = 12.8, p = 0.077, n = 186, Table 2), all the environmental parameters varied among these seven months (Figs. 3–5).

The deficit in rainfall recorded during this period (Fig. 3a), in comparison with the historical means, resulted in more saline waters than observed under typical conditions, which were similar to the drought event, with the highest values being recorded at the end of the El Niño event, that is, in November 2016 (the dry season), when it reached 38.3 ± 5.3 (Fig. 3c). The pH was also relatively high, and the value of 8.3 ± 0.2 was the highest recorded in the study period (Fig. 3d). Turbidity was high (Fig. 3e), but lower than that recorded during the drought, with the highest values being recorded in April 2016 (259.70 ± 142.76 NTU, rainy season). During the El Niño event, the study's highest concentrations of nitrate (4.44 ± 3.49 µmol L^{-1}, September 2016, Fig. 4c), TDN (58.72 ± 14.85, in June 2016, Fig 4e), and silicate (124.8 ± 75.1 µmol L^{-1}, in December 2015, Fig. 4c) were recorded. In fact, the highest pH values, and nitrate, TDN, and silicate concentrations recorded at any time during the study period reached, respectively, mean values of 2%, 30%, 214%, and 35% higher when compared with the typical rainfall conditions of between January 2014 and April 2015.

The rainfall levels recorded during the drought (2012 and 2013) were much lower than those registered during the El Niño event (2015 and 2016). With the exception of salinity (U = 23303,0, p = 0.984, n = 402), DOP (F = 0.005, p = 0.945, n = 402) and chlorophyll-a (F = 0.45, p = 0.500, n = 402), all the environmental parameters varied between these two low-rainfall events (Table 2). In particular, the higher rainfall levels recorded during the first half of 2016 are reflected in the higher concentrations of nitrogenous compounds, i.e., ammonium (2.4 ± 4.5 µmol L^{-1}, Fig. 4a) and nitrate (4.4 ± 3.5

285 µmol L^{-1}, Fig. 4c), in September 2016, in comparison with the same month in 2012 and
286 2013. By contrast, the lower rainfall levels recorded during the first half of 2012 resulted in
287 higher concentrations of phosphorous compounds (Fig. 5a, c) during this year, as shown in
288 the PCA (Fig. 2).

289 The last studied month was April 2017, another typical condition that occurred just
290 after a weak La Niña event. An excess of 11% in rainfall level between December 2016 and
291 March 2017 reflected in shifts in the magnitude of the environmental variables monitored
292 during the study, with either lower or higher values being recorded in comparison with the
293 other studied periods. Comparing the peak rainy season months (March or April) from
294 2012 to 2017, differences were found among periods in all the environmental variables
295 analyzed (Table 2, Figures 3–5). In this scenario, the water of the estuary was less saline
296 (6.2 ± 2.0) and richer in nitrogenous compounds (ammonium, 3.39 ± 1.71 µmol L^{-1}; nitrite:
297 0.90 ± 0.80 µmol L^{-1}; nitrate: 3.91 ± 1.86 µmol L^{-1} and DON: 24.32 ± 20.05 µmol L^{-1}). In
298 fact, the increase in rainfall recorded at the end of 2016 and during the middle of the first
299 half of 2017 when compared to the typical rainy season resulted in a major reduction of
300 salinity (72%), and peaks in turbidity (193%), and in the concentrations of nitrogenous
301 compounds (ammonium: 174%, nitrite 863%, and nitrate 100%) and silicate (42%). By
302 contrast, the phosphorus compounds reached some of their lowest levels (orthophosphate:
303 0.23 ± 0.04 µmol L^{-1}; TDP: 0.29 µmol L^{-1} ± 0.36). Despite the relatively high nutrient
304 concentrations recorded during this period, the chlorophyll-a concentrations were very low
305 (7.3 ± 2.8 mg m^{-3}), influenced by higher turbidity of the water during this period (489.2 ±
306 353.8 NTU).

307 Overall, when rainfall was lower (El Niño and drought), dissolved nutrient
308 concentrations were also slightly lower, although the reduced turbidity of these periods

created ideal conditions for the growth of phytoplankton (as measured by chlorophyll-a concentrations). Conversely, a higher rainfall levels contributed to an increase in nutrient concentrations, in particular of nitrogenous compounds, as recorded during the rainy season of 2017, although, as turbidity also increased, phytoplankton growth was limited.

4. Discussion

Estuarine environments are strongly regulated by climatic conditions, in particular, rainfall levels, which control the input of freshwater into the system and, in turn, the principal physiochemical and hydrobiological variables such as salinity, turbidity, and nutrient and chlorophyll-a concentrations (Arumugam et al. 2016). Given this, large-scale variations in regional climate patterns that determine major fluctuations in rainfall levels are expected to induce extensive impacts on the hydrology and biological productivity of these systems (Wetz et al. 2011; Thompson et al. 2015).

The climate of the Amazon coast is characterized by two main periods, the annual dry and rainy seasons (Martorano et al. 1993). This region is also subject to large scale fluctuations in climate, which modify the normal rainfall pattern. In some cases, these fluctuations induce a decrease in rainfall, which may ultimately result in a drier than normal year (Pereira et al. 2017). This occurs typically under the influence of El Niño or other types of drought conditions. In the opposite scenario, higher than normal rainfall rates are typically associated with the influence of La Niña (Pereira et al. 2013; Andrade et al. 2016). Sixteen of these climate events have been recorded over the past 35 years (Online Resource 1).

The present study did not take spatial variation into account because the Taperaçu is a small estuary (total extension of less than 30 km) with reduced freshwater input, given

333 that its principal input channel has now filled up with sediment (Asp et al. 2012). The small
334 size of the Taperaçu is nevertheless typical of around one third of the estuaries of the
335 Brazilian Amazon coast. Given the lack of any major spatial variation, the present study
336 focused on the patterns of temporal variation associated with the effects of major climate
337 events, an approach adopted by other authors, such as Andrade et al. (2016). The principal
338 temporal patterns observed under each climatic scenario, discussed below, consider in
339 particular the effects of rainfall on the shifts in the salinity of the water, the limitations of
340 the availability of sunlight and nutrients, and their impacts on the phytoplankton biomass.
341
342 4.1 Influence of rainfall on physiochemical variables
343 Located in the equatorial zone, surface water temperatures on the Amazon coast are
344 relatively high and vary by around 2°C (Santos et al., 2008), with no variation between
345 temperature and rainfall (Table 1). On the other hand, salinity presented a systematic
346 pattern of seasonal variation (U = 2258.0, p < 0.001, n = 567, Table 2) and between the
347 different climatic periods (H = 41.51, p < 0.001, n = 567, Table 2), and as expected, a
348 negative correlation was recorded between rainfall and salinity (r_s = -0.84, p < 0.001, n =
349 567, Table 1). During the rainy season, the increased fluvial discharge dominates most of
350 estuaries of the Amazon coast (Asp et al. 2013, 2018), with a subsequent reduction in the
351 salinity of the region's coastal waters, which normally reaches values of 5–10 towards the
352 end of the rainy season, coinciding with the maximum fluvial discharge from the rivers of
353 the coastal plain, as recorded by Pereira et al. (2012) at Princesa beach, 100 km northwest
354 of the present study area, which is dominated by the discharge from the Maracaña and
355 Marapanim rivers. During extreme events of dry climate, as in the drought and El Niño
356 periods, rainfall levels and fluvial discharge may decline, reaching an extreme in the case of

357 estuaries with reduced freshwater input, such as the Taperaçu, where mean salinity reached
358 30 at the end of the rainy season (July in 2013 and 2016, Figure 3b).

359 During the dry season, by contrast, salinity increases and, when evaporation exceeds
360 rainfall levels along the entire Amazon coast, salinity is strongly conditioned by the
361 incursion of seawater into the estuaries, often reaching values of up to 35. Salinity of this
362 level was recorded in the Quatipuru estuary, approximately 30 km northwest of the
363 Taperaçu, by Pamplona et al. (2013) and in the Caeté estuary, 15 km southeast of the
364 Taperaçu, by Asp et al. (2018). In the present study, values of up to 40 were recorded at the
365 end of the dry season during the El Niño event (Fig. 3c). The evaporation and
366 evapotranspiration of the mangrove cause this rapid increase in salinity at the end of the dry
367 season (primarily during drier periods) in small estuaries with little or no freshwater input,
368 as recorded in Northern Australia by Ridd and Stieglitz (2002).

369 During the present study, the highest pH values (7.3–8.3, Fig. 3d) were related
370 closely to the dissolved salt content of the water, given the positive correlation between pH
371 and salinity (r_s = 0.153, p < 0.001, n = 567, Table 1) and the negative correlation with
372 rainfall (r_s = - 0.138, p = 0.001, n = 567, Table 1), rather than to photosynthetic processes
373 (no correlation was found between pH and Chl-a). The freshwater-marine gradient in pH
374 normally ranges from 7.0–7.5 in the more fluvial sectors due to the natural buffering by the
375 carbonate and bicarbonate dissolved in the seawater, as recorded in estuaries in different
376 parts of the world (Krumme et al., 2012; Mansor et al., 2012; Pamplona et al., 2013). As
377 rainfall is the principal source of freshwater in the small Taperaçu estuary, its waters are
378 predominantly alkaline, but when the rainfall is more intense (as in April 2014 and 2017,
379 Fig 3d), the pH is reduced (to a slightly acid condition) together with the salinity. A similar
380 pattern was observed in the Mandovi and Zuari estuaries in India by Saraswat et al. (2015),

where the pH decreased with decreasing salinity during both the monsoon and the post-monsoon seasons.

As expected, the Taperaçu has less turbid waters than estuaries with greater fluvial discharge, such as the Caeté (Asp et al. 2018), with maximum values of 800 NTU being recorded in the rainy season of the typical condition after a La Niña event (Fig. 3e). In fact, the waters of the Amazon coast are turbid, due to the high concentrations of fine suspended particles in the local rivers, as well as the extensive drainage area (Santos et al. 2008; Asp et al. 2016). This results in high levels of turbidity, mainly during the rainy season, when the discharge of the neighboring rivers increases (for example, the Caeté River discharges approximately 180 m^3s^{-1} during this period; Dittmar 1999). This was reflected in the positive correlation between rainfall and turbidity ($r_s = 0.282$, $p < 0.001$, $n = 567$, Table 1), with more turbid waters being recorded during the rainy season ($U = 24769.5$, $p < 0.001$, $n = 567$, Table 2), mainly after a weak La Niña event (Figs. 2a, 3e), while the lowest mean values (< 100 NTU) were recorded at the end of the drought event (Fig. 3e).

A number of natural features contribute to the high dissolved nutrient content of the Amazon coast (Santos et al. 2008; Goes et al. 2014), including the enormous area of the Amazon basin, which is by far the world's most extensive river system, the large area of mangrove forest, which is one of the world's largest continuous mangrove systems, and is flooded regularly by the local macrotides (Souza-Filho 2005; Pereira et al. 2017), the connectivity between estuaries and flooded habitats (Asp et al. 2016), and the local nutrient-rich groundwater (Dittmar 1999). However, what are the effects of different climatic events on the availability of dissolved nutrients?

Comparing typical (2014–2015), drought (2012–2013) and *El Niño* (2015–2016) conditions (Figs. 4-5), differences were found between the dry and rainy seasons in all

dissolved nutrients (Table 2). In fact, a positive correlation was recorded between the nitrogenous compounds and rainfall, whereas there was a negative correlation between phosphorus compounds and rainfall (Table 1), with the highest concentrations of nitrogenous compounds being recorded during the rainy season of the typical condition after a weak La Niña (Figs. 2a, c, 4a-d) and highest phosphorous compounds during the dry season primarily during the drought event (Figs. 2b, c, 5a-c).

While the highest mean value of ammonium was recorded during the rainy season, in particular that of the typical condition after a weak La Niña event (Fig. 4a), this compound was also recorded in high concentrations in the dry season, such as in September 2013 (drought), 2015 (typical) and 2016 (El Niño). This finding may be related to the tidal wash-out of the anoxic interstitial waters of the surface mangrove sediments during high tidal range as recorded in Quatipuru estuary by Pamplona et al. (2013), in Nahoon estuary by Geldenhuys et al. (2016) and in Jiulongjiang estuary by Alongi (2020). In turn, nitrate was the principal nitrogen compound in the rainy season (Fig. 4c). This was likely the result of a combination of the freshwater input from neighboring estuaries and nitrification processes in the water column (Dittmar et al. 2006; Alongi 2013, 2020; Pereira et al. 2013).

By contrast, the orthophosphate and TDP concentrations were clearly related to the influence of marine waters, and correlated strongly with rainfall (orthophosphate: r_s = - 0.439, p < 0.001, n = 567 and TDP: r_s = - 0.401, p < 0.001, n = 567, Table 1), which accounts for the higher values recorded during the dry season, in particular, in December 2012, during the drought (Fig. 5a, c). In shallow estuaries (Z_m < 5 m) - such as the Taperaçu – salinity plays an important role in the release of orthophosphate from particles, reinforcing the possibility of the adsorption-desorption of P from the sediment to the water column as a consequence of the ionic forces related to the increase in salinity recorded

during the drier period when tidal intrusion are intensified in comparation to the rainy season (Turner and Millward 2002; Martin et al. 2008; Pamplona et al. 2013). Oscillations in the orthophosphate concentrations may also be caused by the tidal variation in the input of porewater, which may contribute to the flow of considerable amounts of this compound into coastal waters (Dittmar and Lara 2001a, 2001b; Maslukah et al. 2019), which are generally poorer in nutrients than estuarine waters, in particular during drier periods (Santos et al. 2008; Pereira et al. 2012, 2013).

The strong correlation found between orthophosphate and TDP (r_s = 0.837, p < 0.001, n = 567, Table 1) confirms the association with particles and the increased exchange between the water column and the sediments, primarily during the drier periods, when the intensity of the northeasterly winds increases, and tidal intrusion intensifies (Asp et al., 2012; Pamplona et al. 2013). The values of the DOP reflected a systematic response to rainfall, peaking during the rainy season, in particular in June 2013 (Fig. 5b). However, DON did not show a consistent response to rainfall (no correlation was found between DON and rainfall, table 1).

The mangroves of the estuaries located to the east of the Amazon estuary, which include the Taperaçu, are the principal source of the high concentrations of organic nutrients found in these areas, with around 5 times more DON than DIN (Dittmar and Lara 2001a). In turn, silicate availability is high throughout the Amazon coast and is a result of the input of the adjacent river systems (Pereira et al. 2013), thus presenting a negative correlation with rainfall (r_s = - 0.103, p < 0.014, n = 567, Table 1). This input is combined with that from groundwater sources, which is determined by the variation in the tides, as observed in previous studies, such as that of Dittmar (1999), in an estuary adjacent to the Taperaçu, or in other parts of the world (see Sospedra et al. 2018; Zhang et al. 2020).

453

454 4.2 Effects of salinity, light limitations, and the availability of nutrients on phytoplankton
455 biomass

456 Our results indicate that, when the salinity of water is highest, in particular during
457 the dry season of the drier years (drought and El Niño), chlorophyll-a concentrations are
458 reduced, and are correlated negatively (r_s = - 0.136, p = 0.001, n = 567, Table 1). In fact,
459 salinity varies substantially over a range of time scales, including that of major climate
460 events, driven by fluctuations in precipitation levels, leading to profound shifts in the
461 ecophysiology of phytoplanktonic organisms (Farooq and Siddiqui 2011; Smyth and Elliott
462 2016; Racault et al. 2017), in particular in estuaries of small size that have no direct input
463 of river water, as in the case of the Taperaçu. In the Taperaçu, phytoplankton biomass was
464 affected during December in the drier years, when rainfall was lower than normal, leading
465 to an excess of evapotranspiration and mean salinity of over 37. The chlorophyll-a
466 concentrations were also affected when salinity declined excessively, *i.e.*, when the mean
467 value was less than 7, as observed during the typical rainy seasons.

468 The highest chlorophyll-a concentrations were recorded during March-April in the
469 drier years (drought, typical, and El Niño), when salinity did not decline in the extreme, and
470 the water was less turbid. During these equinoctial periods, the tidal elevation may reach
471 6.0 m, with currents of up to 2.0 m s^{-1} (Pereira et al., 2012; 2013), contributing to a high-
472 energy scenario with the re-suspension of photosynthetic organisms, such as
473 microphytobenthos, and mangrove debris, further contributing to the increase in
474 chlorophyll-a concentrations (Pereira et al. 2010, 2012; Pamplona et al. 2013). In April
475 2017, the greater turbidity (> 400 NTU) was possibly derived from the large quantities of
476 fine sediment and other material derived from the mangrove and adjacent estuaries (Asp et

al. 2018). During this period, rainfall levels were abnormally high, and chlorophyll-a concentrations were very low (Fig. 5e), indicating that phytoplankton growth was also limited by the increased turbidity (Cabeçadas et al. 1999; Burford et al. 2008; Zhou et al. 2012), even though no correlation was found between chlorophyll-a and turbidity.

No correlation was found between the chlorophyll-a concentration and turbidity because high turbidity may often result not only from the resuspension of fine sediments, which normally occur during the peak of the rainy season (when chl-a is low), but also from the resuspension of photosynthetic organisms (normally during equinoctial periods), such as microphytobenthos, as well as debris from the mangrove, which contribute to an increase in chlorophyll-a concentrations. In fact, the highest phytoplankton biomass was recorded when turbidity was between 180 and 220 NTU (Fig 3e).

In general, chlorophyll-a concentrations is reduced during the rainy season, when fluvial discharge increases, and the increased flushing rates and the reduced water residence times prevent the accumulation of biomass within the estuaries (Odebrecht et al. 2015; Du and Shen 2016). Conversely, the absence of any direct fluvial discharge in Taperaçu is one other factor that contributed to the accumulation of phytoplankton biomass within the estuary during the rainy season of the drier years (Asp et al. 2016; Andrade et al. 2016; Pereira et al. 2017).

The nutrient richness of the waters of the Amazon coastal contributes to its high phytoplankton biomass (Pereira et al. 2012, 2013, 2017; Pamplona et al. 2013). While the concentrations of the nitrogenous compounds were correlated with one another, none of these were correlated with the chlorophyll-a concentrations (Table 1). The nutrient richness of the waters of the Amazon coastal contributes to its high phytoplankton biomass (Pereira et al. 2012, 2013, 2017; Pamplona et al. 2013). Except the typical period after a La Niña

event, when turbidity appeared to be the principal factor limiting phytoplankton growth, the increase in the availability of dissolved nitrogenous compounds during the rainy season appeared to contribute to the decrease in the assimilation of phosphorous compounds by the phytoplankton. The N:P ratio of 16.13 recorded during the rainy season was very close to the Redfield ratio (N:P = 16.0), reflecting the balanced availability of these nutrients in the dissolved phase. During this period, even at its lowest levels (N:P = 17.98, El Niño event), phosphorus does not limit phytoplankton growth in the study area. However, a deficit of N was recorded during the dry season, when the N:P ratio (6.66) was much lower than the Redfield ratio, in particular during the drought event (N:P = 3.27).

A positive correlation was found between silicate and chlorophyll-a ($r_s = 0.222$, $p < 0.001$, $n = 567$, Table 1). Silicate compounds are particularly important for the diatoms (the second most abundant algal group), in which they are a component of the valves (Costa et al. 2011; Matos et al. 2011; George et al. 2012; Zhang et al. 2020).

Overall, the results of the present study indicate that the impact of these climate effects is felt immediately in the small study estuary, which has a negligible inflow of freshwater, and where turbidity is the principal variable limiting the accumulation of biomass. The lack of any major input of freshwater also appears to favor the accumulation of phytoplankton biomass in this estuary during the rainy season when turbidity is below 220 NTU.

5. Conclusions

Oscillations in rainfall levels are the principal factor determining the shifts in physicochemical variables, and, in turn, the phytoplankton biomass, but when precipitation decreases, the rainy season of the drier periods is marked by waters that are more saline and

525 richer in orthophosphate and chlorophyll-a. Higher concentrations of nitrogenous
526 compounds were also found during the rainy seasons of the typical period that followed the
527 weak La Niña event, although chlorophyll-a concentrations were lower because turbidity
528 peaked during this period. During the dry seasons of the drier periods, by contrast, even
529 when phosphorous compounds were readily available, phytoplankton biomass was affected
530 by the low levels of nitrogenous compounds. As the waters of the Taperaçu estuary are
531 normally rich in nutrients, high turbidity (> 400 NTU) appears to be the principal
532 physicochemical factors limiting phytoplankton growth. It seems reasonable to expect
533 similar effects in other, similar areas, not only on the Amazon coast, but also in other
534 equivalent estuaries in the equatorial and tropical zones.
535

536 **Acknowledgements**

537 This study was financed by CNPq, through a Universal project (483913/2012-0), and by
538 CAPES (Ciências do Mar II - 88882.158649/2014-01). The authors Pereira LCC
539 (309491/2018-5) and Costa RM (311782/2017-5) would also like to thank CNPq for
540 research grants, and Costa AK and is grateful to CAPES for research grants. We are also
541 indebted to Stephen Ferrari for his careful revision of the English.
542

543 **References**

544 Alongi, D. M. 2013. Cycling and Global Fluxes of Nitrogen in Mangroves. *Global*
545 *Environmental Research*: 173-182.
546 Alongi, D. M. 2020. Nitrogen Cycling and Mass Balance in the World's Mangrove Forests.
547 *Nitrogen*. doi: 10.3390/nitrogen1020014

548 Andrade, M. P., A. Magalhães, L. C. C. Pereira, M. J. Flores-Montes, E. C. Pardal, T. P.
549 Andrade, and R. M. Costa. 2016. Effects of a La Niña event on hydrological patterns and
550 copepod community structure in a shallow tropical estuary (Taperaçu, Northern Brazil).
551 *Journal of Marine System*. doi: 10.1016/j.jmarsys.2016.07.006
552 Araújo Jr, W.P., and N. E. Asp. 2013. Hydrodynamic connectivity between two macrotidal
553 Amazonian estuaries. *Journal of Coastal Research*. doi: 10.2112/SI65-184.1
554 Arumugam, S., S. Sigamani, M. Samikannu, and M. Perumal. 2016. Assemblages of
555 phytoplankton diversity in different zonation of Muthupet mangroves. *Regional Studies in*
556 *Marine Science*. doi: 10.1016/j.rsma.2015.11.005
557 Asp, N. E., C. A. F. Schettini, E. Siegle, M. S. Silva, and R. N. R. Brito. 2012. The
558 Dynamics of a Frictionally-dominated Amazonic Estuary. *Brazilian Journal of*
559 *Oceanography*. doi: 10.1590/S1679-87592012000300011
560 Asp, N. E., P. T. A. Freitas, V. J. C. Gomes, and J. D. Gomes. 2013. Hydrodynamic
561 overview and seasonal variation among the estuarine diversity at the eastern sector of the
562 Amazonian coast. *Journal of Coastal Research*. doi: 10.2112/SI65-185.1
563 Asp, N. E., V. J. C. Gomes, A. Ogston, J. C. C. Borges, and C. A. Nittrouer. 2016.
564 Sediment source, turbidity maximum, and implications for mud exchange between channel
565 and mangroves in an Amazonian estuary. *Ocean Dynamics*. doi: 10.1007/s10236-015-
566 0910-2
567 Asp, N.E., and others. 2018. Sediment dynamics of a tropical tide-dominated estuary:
568 Turbidity maximum, mangroves and the role of the Amazon River sediment load.
569 *Estuarine, Coastal Shelf Science*. doi: 10.1016/j.ecss.2018.09.004
570 Barnard, P. L., and others. 2017. Extreme oceanographic forcing and coastal response due
571 to the 2015–2016 El Niño. *Nature Communications.* doi: 10.1038/ncomms14365

572 Bianchi, T. 2007. *Biogeochemistry of Estuaries*. Oxford University Press.

573 Burford, M. A., D. M. Alongi, A. D. Mckinnon, and L. A. Trott. 2008. Primary production
574 and nutrients in a tropical macrotidal estuary, Darwin Harbour, Australia. *Estuarine,*
575 *Coastal and Shelf Science*. doi: 10.1016/j.ecss.2008.04.018

576 Cabeçadas, G., M. Nogueira, and M. J. Brogueira. 1999. Nutrient dynamics and
577 productivity in three European estuaries. *Marine Pollution Bulletin*. 38 (12): 1092-1096.

578 Callaway, R., S. Grenfell, and C. Lonborg. 2014. Small estuaries: Ecology, environmental
579 drivers and management challenges. *Estuarine Coastal and Shelf Science*. doi:
580 10.1016/j.ecss.2014.06.009

581 Changnon, S. A. 1999. Impacts of 1997–98 El Niño-generated weather in the U.S. *Bulletin*
582 *of the American Meteorological Society.* doi: 10.1175/1520-
583 0477(1999)080<1819:IOENOG>2.0.CO;2

584 Chiew, F. H. A., T. C. Piechota, J. A. Dracup, and T. A. McMahon. 1998. El Niño
585 Southern Oscillation and Australian rainfall, streamflow and drought—links and potential
586 for forecasting. *Journal of Hydrology*. doi:10.1016/S0022-1694(97)00121-2

587 Cohen, M. C. L., R. J. Lara, J. F. D. Ramos, and T. Dittmar. 1999. Factors influencing the
588 variability of Mg, Ca and K in waters of a mangrove creek in Bragança, North Brazil.
589 *Mangroves and Salt Marshes*. doi: 10.1023/A:1009923513091

590 Conover, W. O. J. 1971. *Practical nonparametric statistics*. John Wiley.

591 Costa, K. G., P. R. S. Pinheiro, C. A. R. Melo, S. M. O. Oliveira, L. C. C. Pereira, and R.
592 M. Costa. 2011. Effects of seasonality on zooplankton community dynamics in the
593 macrotidal coastal zone of the Amazon region. *Journal of Coastal Research*. SI: 64: 364-
594 368.

595 Cunha, A. P. M., and others. 2019. Extreme Drought Events over Brazil from 2011 to 2019.
596 *Atmosphere.* doi: 10.3390/atmos10110642
597 DeMaster, D. J., and R. H. Pope. 1996. Nutrient dynamics in Amazon shelf waters: results
598 from AMASSED. *Continental Shelf Research*. doi: 10.1016/0278-4343(95)00008-O
599 Dittmar T. 1999. Nutrient dynamics in a mangrove creek (North Brazil) during dry season.
600 *Mangroves Salt Marsh*. doi: 10.1023/A:1009903824243
601 Dittmar, T., and Lara, R. J. 2001a. Do mangroves rather than rivers provide nutrients to
602 coastal environments south of the Amazon River? Evidence from long-term flux
603 measurements. doi: doi:10.3354/meps213067
604 Dittmar, T., and Lara, R. J. 2001b. Driving Forces Behind Nutrient and Organic Matter
605 Dynamics in a Mangrove Tidal Creek in North Brazil. *Estuarine, Coastal and Shelf*
606 *Science.* doi: 10.1006/ecss.2000.0743
607 Dittmar, T., N. Hertkorn, G. Kattner, and R. J. Lara. 2006. Mangroves, a major source of
608 dissolved organic carbon to the oceans. *Global Biogeochemical Cycles*. doi:
609 10.1029/2005GB002570
610 Du, J., and J. Shen. 2016. Water residence time in Chesapeake Bay for 1980–2012. *Journal*
611 *of Marine Systems*. doi: 10.1016/j.jmarsys.2016.08.011
612 Eltahir, A. B. 1996. El Niño and natural variability in the flow of the Nile River. *Water*
613 *Resource Research*. doi: 10.1029/95WR02968
614 Farooq, S., and P. J. A. Siddiqui. 2011. Distribution of chlorophyll in the mangrove
615 sediments of Sonmiani bay, Pakistan. Pakistan Journal of Botany, 43(1): 405-410.
616 Feng, M., M. J. McPhaden, S-P. Xie, and J. Hafner. 2013. La Niña forces unprecedented
617 Leeuwin Current warming in 2011. *Scientific Reports*. doi: 10.1038/srep01277

618 Francisco, A. S., and S. A. Netto. 2020. El Niño–Southern Oscillations and Pacific
619 Decadal Oscillation as Drivers of the Decadal Dynamics of Benthic Macrofauna in Two
620 Subtropical Estuaries (Southern Brazil). *Ecosystems*. doi: 10.1007/s10021-019-00475-6.
621 Garcia, A. M., J. P. Vieira, K. Winemiller, and A. M. Grimm. 2004. Comparison of the
622 1982-1983 and 1997-1998 El Niño Effects on the Shallow-Water Fish Assemblage of the
623 Patos Lagoon Estuary, Brazil. *Estuaries*. doi: 10.1007/BF02803417
624 Geldenhuys, C., C. Phumlile, and A. Rajkaran. 2016. Understanding the creek dynamics
625 and environmental characteristics that determine the distribution of mangrove and salt
626 marsh communities at Nahoon Estuary. *South African Journal of Botany*. doi:
627 10.1016/j.sajb.2016.04.013
628 George, B., J. I. N. Kumar, and R. N. Kumar. 2012. Study on the influence of hydro-
629 chemical parameters on phytoplankton distribution along Tapi estuarine area of Gulf of
630 Khambhat, *India The Egyptian Journal of Aquatic Research*. doi:
631 10.1016/j.ejar.2012.12.010
632 Geyer, W. R., R. C. Beardsley, S. J. Lentz, J. Candela, R. Limeburner, W. E. Johns, B.M.
633 Castro, and I. D. Soares. 1996. Physical oceanography of the Amazon shelf. *Continental*
634 *Shelf Research.* doi: 10.1016/0278-4343(95)00051-8
635 Goes, J. I., and others. 2014. Influence of the Amazon River discharge on the biogeography
636 of phytoplankton communities in the western tropical north Atlantic. *Progress in*
637 *Oceanography*. doi: 10.1016/j.pocean.2013.07.010
638 Golden Gate Weather Services, 2021. https://ggweather.com/enso/oni.htm
639 Gomez, F. A., F. A. Gomez, S-K Lee, F. J. Hernandez Jr., L. M. Chiaverano, F. E. Muller-
640 Karger, Y. Liu, and J. T. Lamkin. 2019. ENSO-induced co-variability of Salinity,

Plankton Biomass and Coastal Currents in the Northern Gulf of Mexico. *Scientific Reports*. doi: doi: 10.1038/s41598-018-36655-y

Grasshoff, K., M. Ehrhardt, and K. Kremling. 1999. *Methods of Seawater Analysis*. Wiley-VCH.

Grasshoff, K., M. Emrhardt, and K. Kremling. 1983. *Methods of Seawater Analysis*. Verlag Chemie.

Grimm, A. M., S. E. T. Ferraz, and J. Gomes. 1998. Precipitation anomalies in Southern Brazil associated with El Niño and La Niña events. *Journal of Climate*. doi: 10.1175/1520-0442(1998)011<2863:PAISBA>2.0.CO;2

Grimm, A. M., V. R. Barros, and M. E. Doyle. 2000. Climate variability in southern South America associated with El Niño and La Niña events. *Journal of Climate.* doi: 10.1175/1520-0442(2000)013<0035:CVISSA>2.0.CO;2

Instituto Nacional de Meteorologia (INMET). 2019. Monitoramento das estações automáticas. http://www.inmet.gov.br/sonabra/maps/automaticas.php. Accessed between 1st March and 1st October 2019.

Kjerfve, B., and L. D. Lacerda. 1993. Mangroves of Brazil. In *Conservation and Sustainable Utilization of Mangrove Forests in Latin America and Africa Regions*, *Part I. Latin America*, ed. L. D. Lacerda, 245–272. ITTO/ International Society for Mangrove Ecosystems.

Krause G, D. Schories, M. Glaser, and K. Diele. 2001. Spatial patterns of mangrove ecosystems: the bragantinian mangroves of North Brazil (Bragança, Pará). *Ecotropica*. 7: 93-107.

663 Krumme U., L. S. Herbeck, and Wang T. 2012. Tide- and rainfall-induced variations of
664 physical and chemical parameters in a mangrove-depleted estuary of East Hainan (South
665 China Sea). *Marine Environmental Research*. 82:28-39.
666 Legendre, P. and L. Legendre. 2012. Numerical Ecology. Third English Edition. Elsevier.
667 Mansor M. I., M. Z. Mohammad-Zafrizal, M. A. Nur-Fadhilah, Y. Khairun, and W. O.
668 Wan-Maznah. 2012. Temporal and Spatial Variations in Fish Assemblage Structures in
669 Relation to the Physicochemical Parameters of the Merbok Estuary, Kedah. *Journal of*
670 *Natural Sciences Research*. 2: 7.
671 Marengo, J. A., J. Tomasella, L. M. Alves, W. Soares, and D. A. Rodriguez. 2011. The
672 drought of 2010 in the context of historical droughts in the Amazon region. *Geophysical*
673 *Research Letter*. doi: 10.1029/2011GL047436
674 Marengo, J. A., J. Tomasella, W. R. Soares, L. M. Alves, and C. A. Nobre. 2012. Extreme
675 climatic events in the Amazon basin: climatological and hydrological context of recent
676 floods. *Theoretical and Applied Climatology*. doi: 10.1007/s00704-011-0465-1
677 Marengo, J. A., L. M. Alves, W. R. Soares, D. A. Rodriguez, H. Camargo, M. P. Riveros,
678 and A. D. Pabló. 2013a. Two Contrasting Severe Seasonal Extremes in Tropical South
679 America in 2012: Flood in Amazonia and Drought in Northeast Brazil. *Journal of Climate*.
680 doi: 10.1175/JCLI-D-12-00642.1
681 Marengo, J. A., L. S. Borma, D. A. Rodriguez, P. Pinho, W. R. Soares, and L. M. Alves.
682 2013b. Recent Extremes of Drought and Flooding in Amazonia: Vulnerabilities and Human
683 Adaptation. *American Journal of Climate Change*. doi: 10.4236/ajcc.2013.22009
684 Marengo, J. A., R. T. Roger, and M. A. Lincoln. 2016. Drought in Northeast Brazil—past,
685 present, and future. *Theoretical and Applied Climatology*. doi: 10.1007/s00704-016-1840-
686 8

687 Marengo, J.A., C.A. Nobre, J. Tomasella, M. Oyama, G. Sampaio, H. Camargo, and L.
688 Alves. 2008. The Drought of Amazonia in 2005. *Journal of Climate.* doi:
689 10.1175/2007JCLI1600.1
690 Martin, G. D., J. G. Vijay, C. M. Laluraj, N.V. Madhu, T. Joseph, M. Nair, G.V.M. Gupta,
691 K.K., Balachandran. 2008. Fresh water influence on nutrient stoichiometry in a tropical
692 estuary, southwest coast of India. *Applied Ecololy and Environmental Research.* 6(1): 57-
693 64.
694 Martorano, L. G., L. C., Pereira, E. G. M., Cezar, and I. C. B., Pereira, 1993. *Estudos*
695 *Climáticos do Estado do Pará, Classificação Climática (KÖPPEN) e Deficiência Hídrica*
696 *(Thornthwhite, Mather)*. SUDAM/EMBRAPA, SNLCS, Belém.
697 Maslukah L., S. Y. Wulandari, I. B. Prasetyawan, and M. Zainuri. 2019. Distributions and
698 Fluxes of Nitrogen and Phosphorus Nutrients in Porewater Sediments in the Estuary of
699 Jepara Indonesia. *Journal of Ecological Engineering.* doi:10.12911/22998993/95093
700 Matos, J. B., D. K. L. Sodré, K. G. Costa, L. C. C. Pereira, and R. M. Costa. 2011. Spatial
701 and temporal variation in the composition and biomass of phytoplankton in an Amazon
702 estuary. *Journal of Coastal Research.* SI 64: 1525-1529.
703 Menezes, M. P. M., U. Berger, and U. Mehlig. 2008. Mangrove vegetation in Amazonia: a
704 review of studies from the coast of Pará and Maranhão States, north Brazil. *Acta*
705 *Amazônica*. doi: 10.1590/S0044-59672008000300004
706 Milligan, G. W., and M. C. Cooper. 1988. A study of standardization of variables in cluster
707 analysis. *Journal of Classification*. doi: 10.1007/BF01897163
708 Moeletsi, M. E., S., Walker, and W. A. Landman. 2011. ENSO and implications on rainfall
709 characteristics with reference to maize production in the Free State Province of South
710 Africa. *Physics and Chemistry of the Earth, Parts A/B/C*. doi: 10.1016/j.pce.2011.07.043

711 Odebrecht, C., P. C. Abreu, and J. Carstensen. 2015. Retention time generates short-term
712 phytoplankton blooms in a shallow microtidal subtropical estuary. *Estuarine, Coastal and*
713 *Shelf Science*. doi: 10.1016/j.ecss.2015.03.004
714 Palutikof J. P., S. L. Boulter, J. Barnett, and D. Rissik. 2015. *Applied Studies in Climate*
715 *Adaptation*. Willey Blackwell.
716 Pamplona, F. C., E. T. Paes, and A. Nepomuceno. 2013. Nutrient fluctuations in the
717 Quatipuru river: A macrotidal estuarine mangrove system in the Brazilian Amazonian
718 basin. *Estuarine, Coastal and Shelf Science*. doi: 10.1016/j.ecss.2013.09.010
719 Parsons, T. R., and J. D. H. Strickland. 1963. Discussion of spectrophotometric
720 determination of marine plant pigments with revised equations of ascertaining chlorophyll-
721 a and carotenoids. *Journal of Marine Research*, 21: 155-163.
722 Pereira, L. C. C., A. K. R. Costa, R. M. Costa, A. Magalhães, and M. J. A. Flores-Montes.
723 2017. Influence of a Drought Event on Hydrological Characteristics of a Small Estuary on
724 the Amazon Mangrove Coast. *Estuaries and Coasts*. doi: 10.1007/s12237-017-0310-6
725 Pereira, L. C. C., M. C. Monteiro, D. O. Guimarães, J. B. Matos, and R. M. Costa. 2010.
726 Seasonal effects of wastewater to the water quality of the Caeté river estuary, Brazilian
727 Amazon. *Anais da Academia Brasileira de Ciências*. doi: 10.1590/S0001-
728 37652010000200022
729 Pereira, L. C. C., N. I. S. Silva, R. M. Costa, N. E. Asp, K. G. Costa, and A. Vila-Concejo.
730 2012. Seasonal changes in oceanographic processes at an equatorial macrotidal beach in
731 northern Brazil. *Continental Shelf Research*. doi: 10.1016/j.csr.2012.05.003
732 Pereira, L. C. C., S. M. O. Oliveira, R. M. Costa, K. G. Costa, and A. Vila-Concejo. 2013.
733 What happens on an equatorial beach on the Amazon coast when La Niña occurs during the
734 rainy season? *Estuarine, Coastal and Shelf Science*. doi: 10.1016/j.ecss.2013.07.017

735 Racault M. F., Sathyendranath S., Brewin R. J. W., Raitsos D. E., Jackson T., and Platt T.
736 2017. Impact of El Niño Variability on Oceanic Phytoplankton. *Frontiers in Marine*
737 *Science*. doi: 10.3389/fmars.2017.00133
738 Restrepo, J. C., J. C. Ortíz, J. Pierini, K. Schrottke, M. Maza, L. Otero, and J. Aguirre.
739 2014. Freshwater discharge into the Caribbean Sea from the rivers of Northwestern South
740 America (Colombia): Magnitude, variability and recent changes. *Journal of Hydrology*.
741 doi: 10.1016/j.jhydrol.2013.11.045
742 Ridd, P.V., and T. Stieglitz. 2002. Dry Season Salinity Changes in Arid Estuaries Fringed
743 by Mangroves and Saltflats. *Estuarine, Coastal and Shelf Science*. doi:
744 10.1006/ecss.2001.0876
745 Rossi, S., and M. O. Soares. 2017. Effects of El Niño on the coastal ecosystems and their
746 related services. *Mercator*. doi: 10.4215/rm2017.e16030
747 Santos, M. L. S., C. Medeiros, M. Muniz, M. L. S. Feitosa, R. Schwamborn, and S. J.
748 Macedo. 2008. Influence of the Amazon and Pará Rivers on water composition and
749 phytoplankton biomass on the adjacent shelf. *Journal of Coastal Research*. doi:
750 10.2112/05-0538.1
751 Saraswat R., M. Kouthanker, S. R. Kurtarkar, R. Nigam, S.W.A. Naqvi, and V.N. Linshy.
752 2015. Effect of salinity induced pH/alkalinity changes on benthic foraminifera: A
753 laboratory culture experiment. *Estuarine, Coastal and Shelf Science*. doi:
754 10.1016/j.ecss.2014.12.005
755 Siegert, M. J., and I. Marsiat. 2001. Numerical reconstructions of LGM climate across the
756 Eurasian Arctic. *Quaternary Science Reviews*. doi: 10.1016/S0277-3791(01)00017-8
757 Smyth, K., and M. Elliott. 2016. Effects of changing salinity on the ecology of the marine
758 environment. doi:10.1093/acprof:oso/9780198718826.003.0009

759 Sospedra, J., L. F. H. Niencheski, S. Falco, C. F. F. Andrade, K. K. Attisano, and M.
760 Rodilla, 2018. Identifying the main sources of silicate in coastal waters of the Southern
761 Gulf of Valencia (Western Mediterranean Sea). *Oceanologia*. doi:
762 10.1016/j.oceano.2017.07.004.
763 Souza-Filho, P. W. M. 2005. Costa de manguezais de macromaré da Amazônia: cenários
764 morfológicos, mapeamento e quantificação de áreas usando dados de sensores remotos.
765 *Revista Brasileira de Geofísica*. doi: 10.1590/S0102-261X2005000400006
766 Strickland, J. D. H., and T. R. Parsons. 1972. *A Practical Handbook of Seawater Analysis*.
767 2nd edition. Fisheries Research Board of Canada, Otawa.
768 Ter Braak, C.J.F., and P. Smilauer. 2002. *CANOCO Reference Manual and CanoDraw for*
769 *Windows User's Guide: Software for Canonical Community Ordination (Version 4.5).*
770 *Microcomputer Power*, New York.
771 Thompson, P. A. P. Bonham, P. Thomson, W. Rochester, M. A. Doblin, A. M. Waite, A.
772 Richardson, and C. S. Rousseaux. 2015. Climate variability drives plankton community
773 composition changes: the 2010–2011 El Niño to La Niña transition around Australia.
774 *Journal of Plankton Research.* doi: 10.1093/plankt/fbv069.
775 Turner, A., and G. E. Millward. 2002. Suspended particles: their role in estuarine
776 biogeochemical cycles. *Estuarine, Coastal and Shelf Science*. doi: 10.1006/ecss.2002.1033
777 UNESCO, 1996. *Monograph on Oceanographic Methodology. I. Determination of*
778 *Photosynthetic Pigments in Sea Water*. United Nations Education, Science, and Culture
779 Organization, Paris.
780 Valiela, I., A. A. Giblin, C. Barth-Jensen, C. Harris, T. Stone, S. Fox, and J. Crusius. 2013.
781 Nutrient gradients in Panamanian estuaries: effects of watershed deforestation, rainfall,

782 upwelling, and within-estuary transformations. *Marine Ecology Progress Series*. doi:
783 10.3354/meps10358
784 Valiela, I., and others. 2012. Increased rainfall remarkably freshens estuarine and coastal
785 waters on the Pacific coast of Panama: Magnitude and likely effects on upwelling and
786 nutrient supply. *Global and Planetary Change*. doi: 10.1016/j.gloplacha.2012.05.006
787 Wetz, M. S., E. A. Hutchinson, R. S. Lunetta, H. W. Paerl, and J. C. Taylor. 2011. Severe
788 droughts reduce estuarine primary productivity with cascading effects on higher trophic
789 levels. *Limnology and Oceanography*. doi: 10.4319/lo.2011.56.2.0627
790 Wilkerson, F. P., R. C. Dugdale, A. Marchi, and C. A. Collins. 2002. Hydrography,
791 nutrients and chlorophyll during El Niño and La Niña 1997–99 winters in the Gulf of the
792 Farallones, California. *Progress in Oceanography*. doi: 10.1016/S0079-6611(02)00055-1
793 Xue, Y., and A. Kumar. 2016. Evolution of the 2015/16 El Niño and historical
794 perspective since 1979. *Science China Earth Sciences*. doi: 10.1007/s11430-016-0106-9
795 Zar, J. H. 1999. *Biostatistical Analysis*. New Jersey: Prentice Hall.
796 Zaroug, M. A. H., E. A. B., Eltahi, and F. Giorgi. 2014. Droughts and floods over the upper
797 catchment of the Blue Nile and their connections to the timing of El Niño and La Niña
798 events. *Hydrology and Earth System Sciences*. doi: 10.5194/hess-18-1239-2014
799 Zhang, P., J-L Xu, J-B Zhang, J-X Li, Y-C Zhang, Y. Li, and X-Q Luo. 2020.
800 Spatiotemporal Dissolved Silicate Variation, Sources, and Behavior in the Eutrophic
801 Zhanjiang Bay, China. *Water*. doi: 10.3390/w12123586
802 Zhou, G., X. Zhao, Y. Bi, and Z. Hu. 2012. Effects of rainfall on spring phytoplankton
803 community structure in Xiangxi Bay of the Three-Gorges Reservoir, China. *Fresenius*
804 *Environmental Bulletin.* 21(11c): 3533-3541
805

Figure Caption

Figure 1. Study area, showing the South America (a) Brazilian Amazon coast (b) and the Taperaçu Estuary with the three sampling stations S1-S3 (c).

Figure 2. Graphical representation of the factorial plan of the first and second axes of the principal component analysis (PCA) of the data from: (a) dry season; circles, (b) rainy season; square, (c) vector ordering diagram of the environmental variables in the PCA factorial plane.

Figure 3. Means and (positive) standard deviations recorded for cumulative 3-month (February-April) rainfall level (a), water temperature (b), salinity (c), turbidity (d), pH (e), and cumulative rainfall every three months. The gray hatching represents the rainy season. Typ typical.

Figure 4. Means and (positive) standard deviations recorded for ammonium (a), nitrite (b), nitrate (c), DON (d) and total dissolved nitrogen (e), and cumulative rainfall every three months. The gray hatching represents the rainy season. Typ typical.

Figure 5. Means and (positive) standard deviations recorded for orthophosphate (a), DOP (b), total dissolved phosphorus (c), silicate (d), and chlorophyll-a (e), and cumulative rainfall every three months. The gray hatching represents the rainy season. Typ typical.

Figure 1

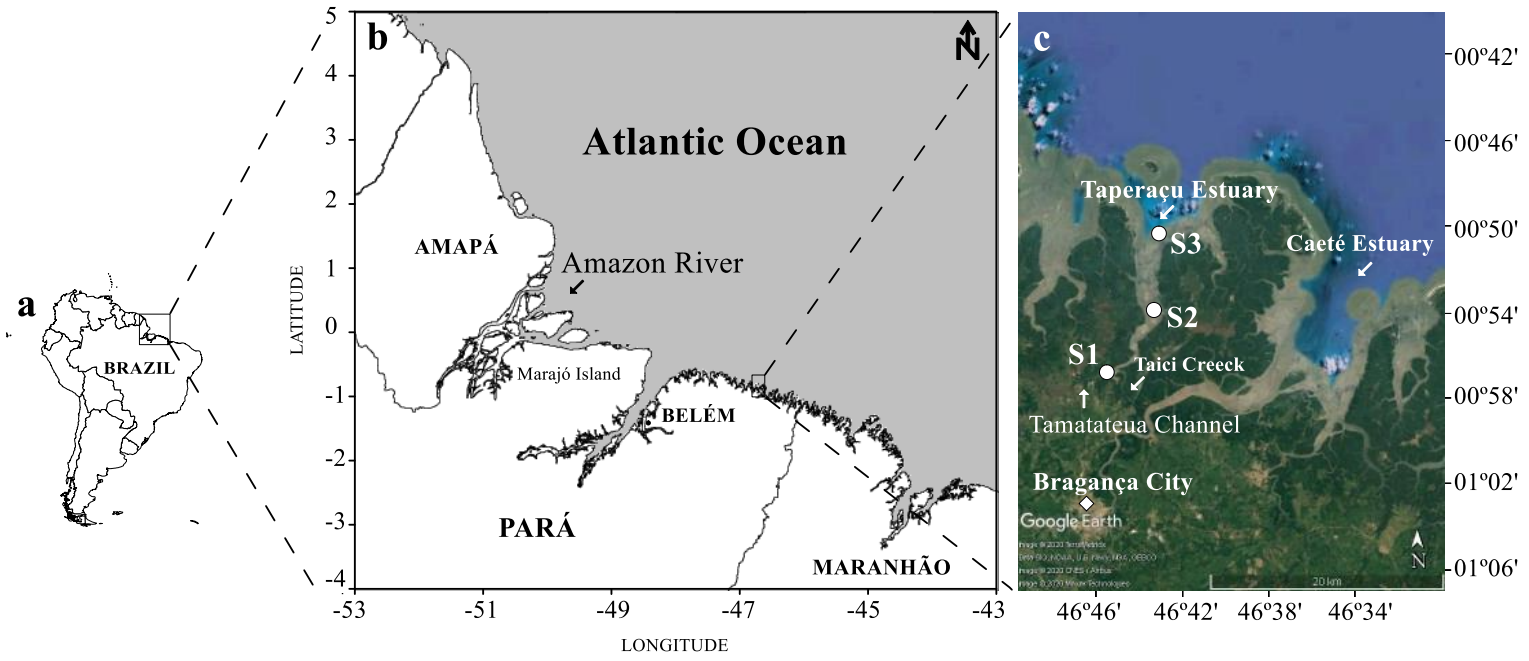
a
BRAZIL
b
Atlantic Ocean
AMAPÁ
Amazon River
Marajó Island
BELÉM
PARÁ
MARANHÃO
LATITUDE
LONGITUDE
5
4
3
2
1
0
-1
-2
-3
-4
-53
-51
-49
-47
-45
-43
c
Taperaçu Estuary
S3
Caeté Estuary
S2
S1
Taici Creeck
Tamatateua Channel
Bragança City
Google Earth
20 km
00°42'
00°46'
00°50'
00°54'
00°58'
01°02'
01°06'
46°46'
46°42'
46°38'
46°34'

Figure 2

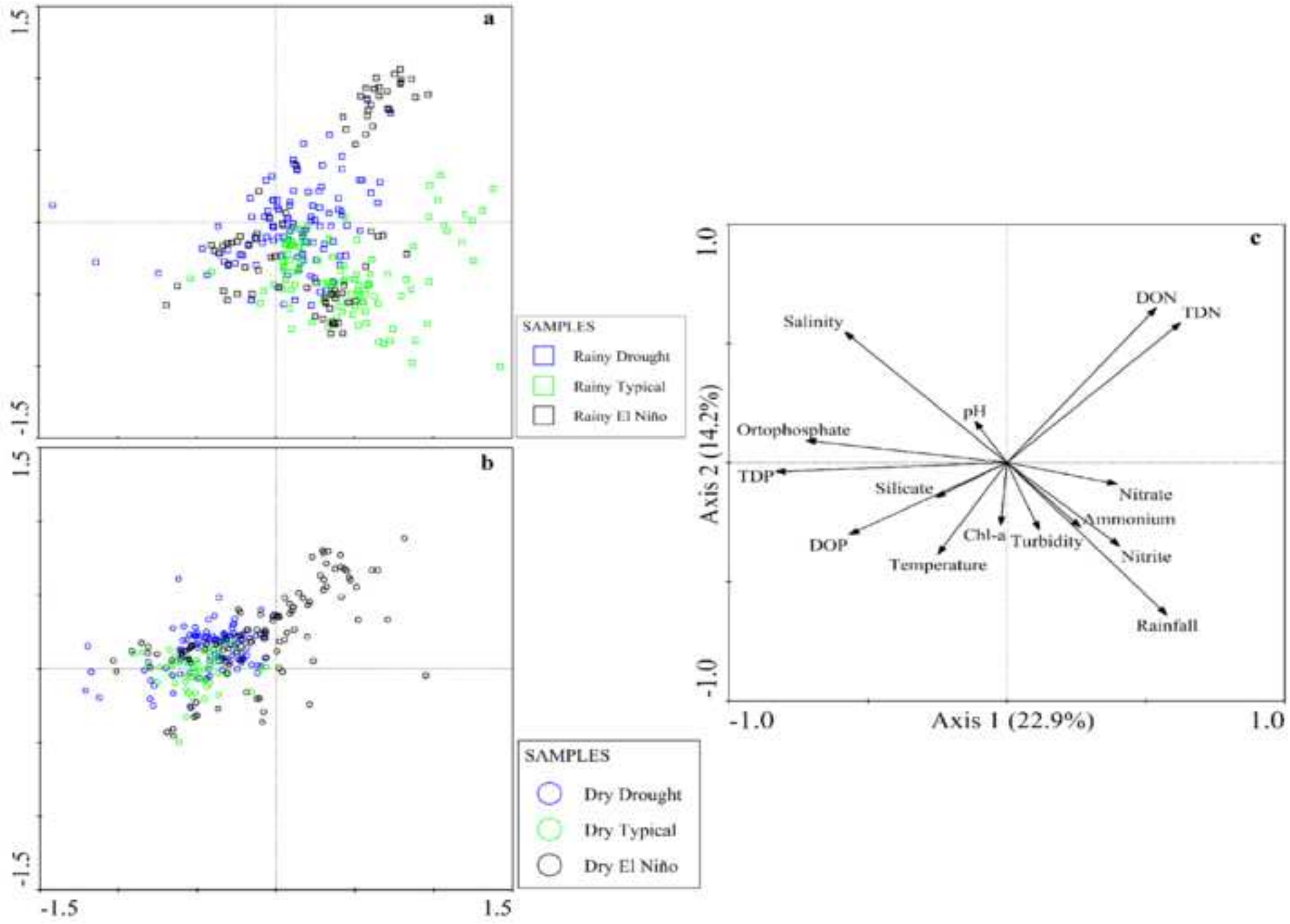

Figure 3

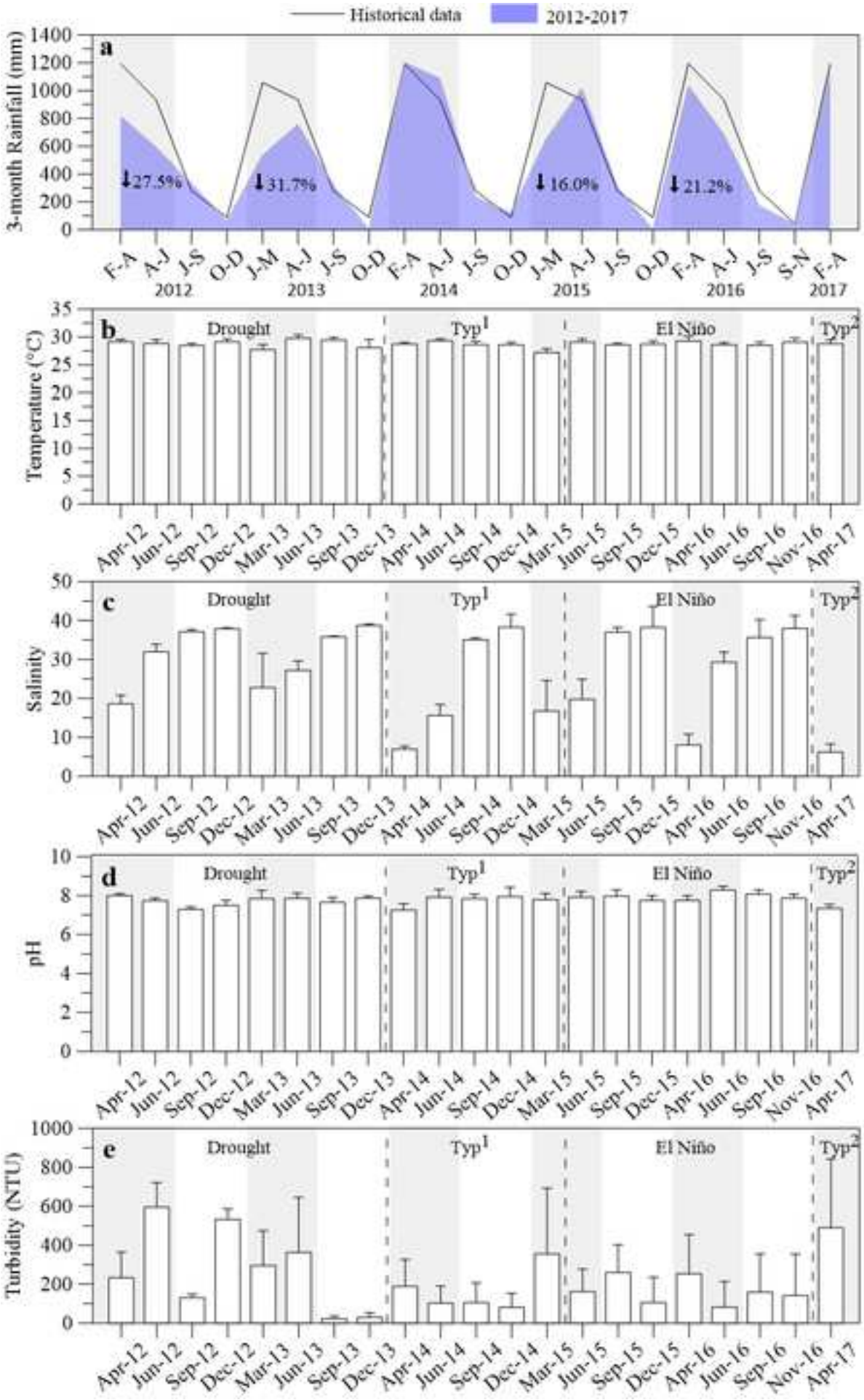

Figure 4

Click here to access/download;Figure;Figure4ESCOR2.tif

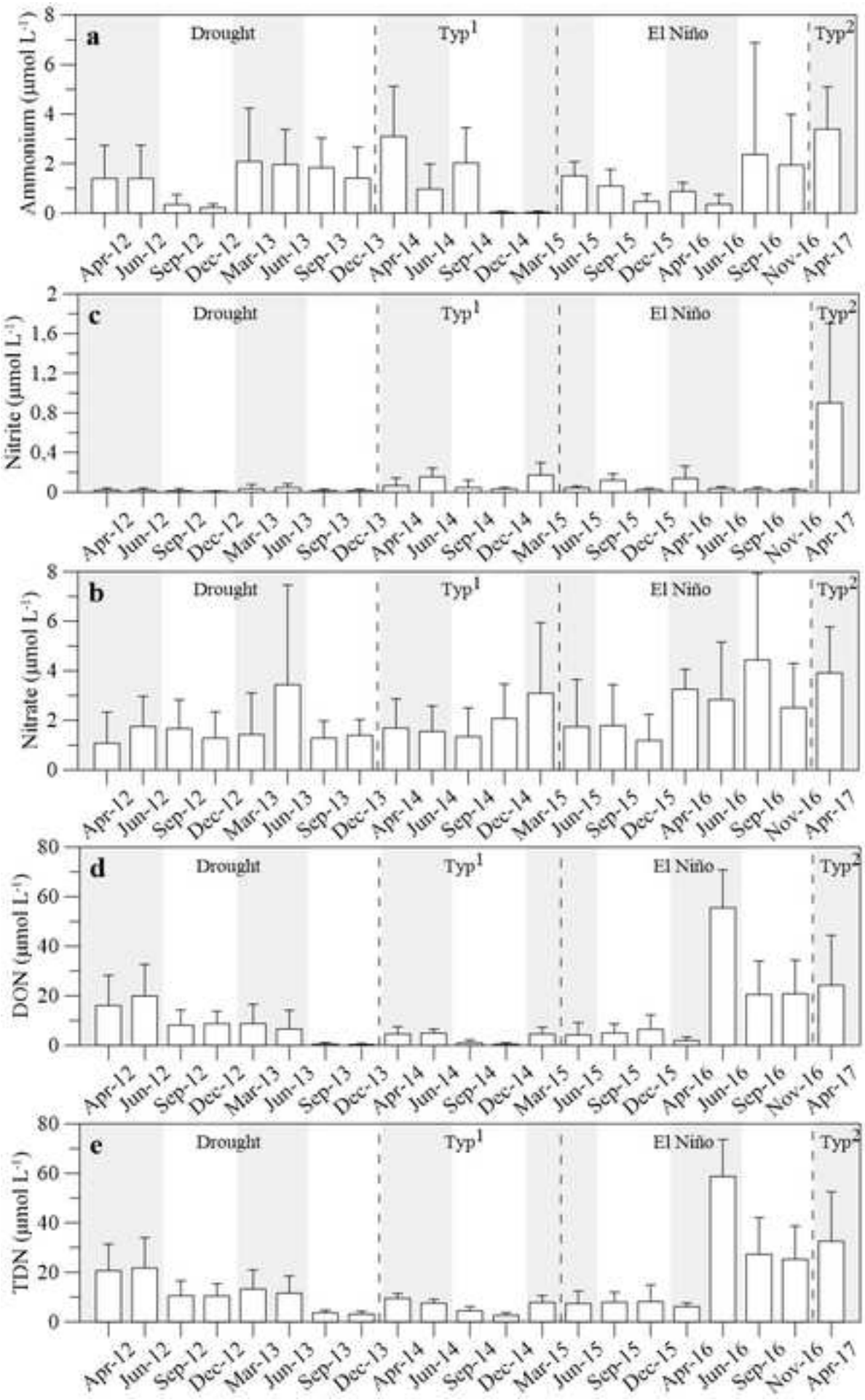

Figure 5

Click here to access/download;Figure;Figure5ESCOR2.tif

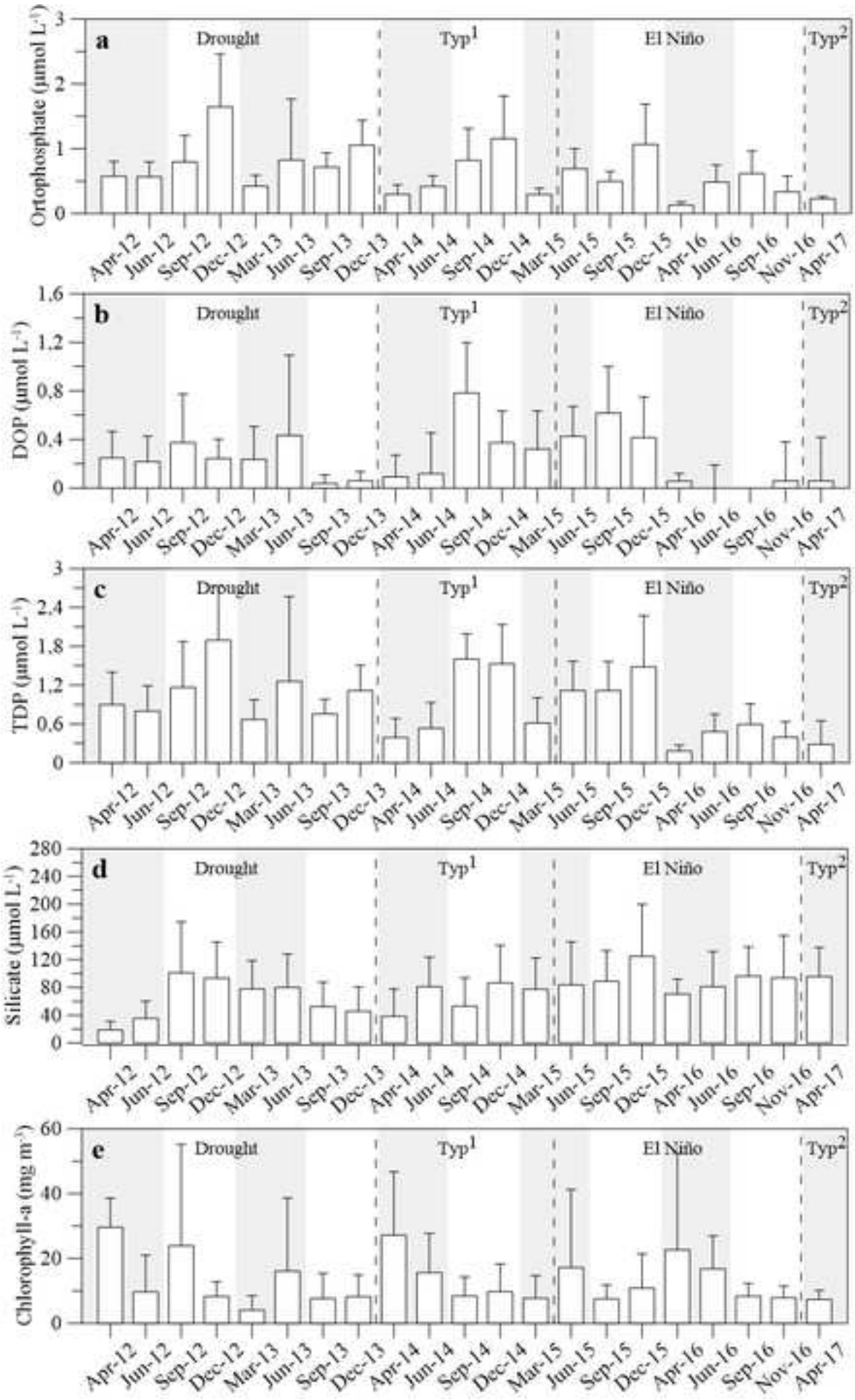

Table 1

Table 1. Matrix of Spearman correlation between environmental variables in the Taperaçu estuary, northern Brazil, during the field campaigns conducted in the present study. Temp = Temperature, Sal = Salinity, Turb = Turbidity, Chl-a = Chlorophyll-a.

Variables		Rainfall	Temp	Sal	Turb	pH	NH_4^+	NO_2^-	NO_3^-	DON	TDN	PO_4^{3-}	DOP	TDP	DSi
Temp	r_s	0.061													
	p	0.147													
Sal	r_s	-0.840	-0.120												
	p	0.000	0.004												
Turb	r_s	0.282	-0.004	-0.316											
	p	0.000	0.925	0.000											
pH	r_s	-0.138	-0.020	0.153	-0.228										
	p	0.001	0.641	0.000	0.000										
NH_4^+	r_s	0.121	0.183	-0.237	0.062	-0.078									
	p	0.004	0.000	0.000	0.138	0.065									
NO_2^-	r_s	0.379	-0.007	-0.448	0.150	0.034	0.100								
	p	0.000	0.876	0.000	0.000	0.420	0.018								
NO_3^-	r_s	0.170	-0.009	-0.188	0.036	0.000	0.078	0.194							
	p	0.000	0.833	0.000	0.399	0.994	0.063	0.000							
DON	r_s	0.006	-0.056	-0.111	0.224	0.076	-0.006	0.035	0.090						
	p	0.884	0.0179	0.008	0.00	0.072	0.000	0.408	0.032						
TDN	r_s	0.107	-0.031	-0.228	0.248	0.042	0.215	0.117	0.353	0.890					
	p	0.011	0.459	0.000	0.000	0.316	0.000	0.005	0.000	0.000					
PO_4^{3-}	r_s	-0.439	0.000	0.484	-0.074	-0.083	-0.131	-0.366	-0.275	-1.603	-0.257				
	p	0.000	0.997	0.000	0.080	0.047	0.002	0.000	0.000	0.000	0.000				
DOP	r_s	-0.158	-0.054	0.168	0.073	0.044	-0.073	-0.074	-0.205	-0.158	-0.236	0.308			
	p	0.000	0.197	0.000	0.082	0.295	0.080	0.076	0.000	0.000	0.000	0.000			
TDP	r_s	-0.401	-0.054	0.437	-0.027	-0.056	-0.127	-0.270	-0.321	-0.241	-0.345	0.837	0.719		
	p	0.000	0.203	0.000	0.515	0.182	0.002	0.00	0.000	0.000	0.000	0.000	0.000		
DSi	r_s	-0.103	0.011	0.065	0.120	-0.103	-0.079	0.192	0.074	0.080	0.069	0.356	0.099	0.283	
	p	0.014	0.798	0.121	0.004	0.014	0.060	0.000	0.078	0.057	0.102	0.000	0.018	0.000	
Chl-a	*rs*	0.111	0.104	-0.136	0.026	-0.021	0.053	0.042	0.029	0.151	0.150	0.173	0.013	0.114	0.222
	p	0.008	0.013	0.001	0.530	0.613	0.208	0.314	0.487	0.000	0.000	0.000	0.757	0.007	0.000

Table 2

Table 2. Analysis of variability of hydrological parameters for different time (climatic) periods. The temporal scales were evaluated by ANOVA (*F*) or the Mann-Whitney *U* and Kruskal-Wallis *H* tests. If the ANOVA or Kruskal-Wallis test indicated significant variation among seasons or months, *a posteriori* pairwise Fisher's LSD (ANOVA) or Student-Newman-Keuls (Kruskal-Wallis) tests were run. The interactions of seasonal *vs* events were assessed by a two-way ANOVA. DRY Dry, RAI Rainny, D Drought, EN El Niño, T Typical.

Variables	**Typical conditions (n=270)**	**Drought event (n=216)**	**El Niño event (n=186)**	**Drought/ El Niño (=402)**	**Mar/Apr Months (n=54)**	**Seasonal (1) (n=567)**	**Climatic event (2) (n=567)**	**1x2**
Temperature	*H*=32.8	*H*=100.3	*H*=89.0	*U* = 19376.0	*H*=86.5	DRY RAI	D T EN	*F* = 0.93
	p = 0.000	*p* = 0.000	*p* = 0.000	*p* = 0.002	*p* = 0.000	*U* = 34991.0, *p* = 0.009	*H* = 11.21, *p* = 0.004	*p* = 0.393
Salinity	*H*=119.5	*H*=149.1	*H*=176.6	*U* = 23303.0	*H*=85.2	DRY RAI	D EN T	*F* = 71.74
	p = 0.000	*p* = 0.000	*p* = 0.000	*p* = 0.985	*p* = 0.000	*U* = 2258.0, *p* = 0.000	*H* = 41.51, *p* = 0.000	*p* = 0.000
pH	*H*=61.5	*H*=109.4	*H*=77.9	*F* = 57.1	*H*=80.9	DRY RAI	D EN T	*F* = 42.84
	p = 0.000	*p* = 0.000	*p* = 0.000	*p =0.000*	*p* = 0.000	*F* = 34.3, *p* = 0.000	*H* = 66.7, *p* = 0.000	*p* = 0.000
Turbidity	*F*=18.3	*H*=156.9	*F*=10.4	*F = 4.35*	*F* = 2.2	DRY RAI	D EN T	*F* = 0.92
	p = 0.000	*p* = 0.000	*p* = 0.000	*p = 0.037*	*p* = 0.0058	*U* = 24769.5, *p* = 0.000	*H* = 27.3, *p* = 0.000	*p* = 0.400
Ammonium	*H*=79.6	*H*=98.5	*H*=130.8	*U = 18623.0*	*H*=94.5	DRY RAI	D T EN	*F* = 1.21
	p = 0.000	*p* = 0.000	*p* = 0.000	*p = 0.000*	*p* = 0.000	*F* = 13.62, *p* = 0.000	*F* = 13.64, *p* = 0.001	*p* = 0.292
Nitrite	*H*=78.1	*H*=40.8	*H*=97.9	*U = 12268.5*	*H*=72.9	DRY RAI	D T EN	*F* = 25.30
	p = 0.000	*p* = 0.000	*p* = 0.000	*p =0.000*	*p* = 0.000	*F* = 11.19, *p* = 0.000	*H* = 17.67, *p* = 0.000	*p* = 0.000
Nitrate	*F* = 4.0	*H*=22.1	*H*=44.4	*U = 18743.5*	*H*=36.2	DRY RAI	D T EN	*F* = 20.48
	p = 0.005	*p* = 0.005	*p* = 0.000	*p = 0.000*	*p* = 0.000	*U* = 32203.0, *p* = 0.000	*H* = 105.6, *p* = 0.000	*p* = 0.000
DON	*H* = 71.3	*H* = 126.5	*H* = 129.6	*F = 10.59*	*H* = 48.0	DRY RAI	D T EN	*F* = 2.99
	p = 0.000	*p = 0.000*	*p* = 0.000	*p = 0.001*	*p* =0.000	*F* = 36.83, *p* = 0.000	*F* = 16.50, *p* = 0.000	*p* = 0.051
TDN	*H = 105.9*	*H*=126.3	*H*=127.8	*U = 19895.0*	*H*=84.0	DRY RAI	D T EN	*F* = 4.63
	p = 0.000	*p* = 0.000	*p* = 0.000	*p = 0.008*	*p* = 0.000	*F* = 67.80, *p* = 0.000	*H* = 18.79, *p* = 0.000	*p* = 0.010
Ortophosphate	*H*=84.5	*H*=87.0	*H*=117.4	*U = 13756.0*	*H*=40.9	DRY RAI	D T EN	*F* = 7.61
	p = 0.000	*p* = 0.000	*p* = 0.000	*p = 0.000*	*p* = 0.000	*U* = 18808.0, *p* = 0.000	*H* = 62.64, *p* = 0.000	*p* = 0.001
POD	*F* = 34.0	*H = 67.6*	*H* = 92.1	*F = 0.005*	*H* = 51.4	DRY RAI	D EN T	*F* = 30.32
	p = 0.000	*p* = 0.000	*p* = 0.000	*p = 0.945*	*p* = 0.000	*U* = 32191.0, *p* = 0.000	*F* = 1.60, *p* = 0.450	*p* = 0.000
TDP	*F*=87.0	*H*=62.4	*H*=125.2	*U = 16298.5*	*H*=79.3	DRY RAI	D T EN	*F* = 20.98
	p = 0.000	*p* = 0.000	*p* = 0.000	*p = 0.000*	*p* = 0.000	*F* = 121.84, *p* = 0.000	*H* = 14.40, *p* = 0.000	*p* = 0.000
Silicate	*F*=8.1	*F*=6.6	*H*=12.8	*F = 22.3*	*H*=92.7	DRY RAI	D T EN	*F* = 2.59
	p = 0.000	*p* = 0.000	*p* = 0.077	*p = 0.000*	*p* = 0.000	*F* = 5.62, *p* = 0.000	*F* = 12.38, *p* = 0.000	*p* = 0.076
Chlorophyll-a	*H*=22.5	*H*=73.8	*H*=30.3	*F = 0.45*	*H*=76.0	DRY RAI	D EN T	*F* = 1.51
	p = 0.000	*p* = 0.000	*p* = 0.000	*p = 0.500*	*p* = 0.000	*U* = 33158.5, *p* = 0.000	*H* = 4.03, *p* = 0.133	*p* = 0.221

Electronic Supplemental Material

Effects of extreme climatic events on the hydrological parameters of the estuarine waters of the Amazon Coast

Ádila Kelly Rodrigues da Costa[1], Luci Cajueiro Carneiro Pereira[1,*], José A. Jiménez[2], Antonio Rafael Gomes de Oliveira[1], Manuel de Jesus Flores-Montes[3] and Rauquírio Marinho da Costa[1]

[1]Universidade Federal do Pará, Instituto de Estudos Costeiros, Alameda Leandro Ribeiro sn, Aldeia, 68600-000, Braganca-Pará. *E-mail: cajueiro@ufpa.br.
[2]Universitat Politècnica de Catalunya - BarcelonaTech, Laboratori d'Enginyeria Marítima, C/Jordi Girona, 1-3, 08034, Barcelona, Spain.
[3]Universidade Federal de Pernambuco, Departamento de Oceanografia, Avenida Arquitetura, s/n, Cidade Universitária, Recife, Pernambuco.

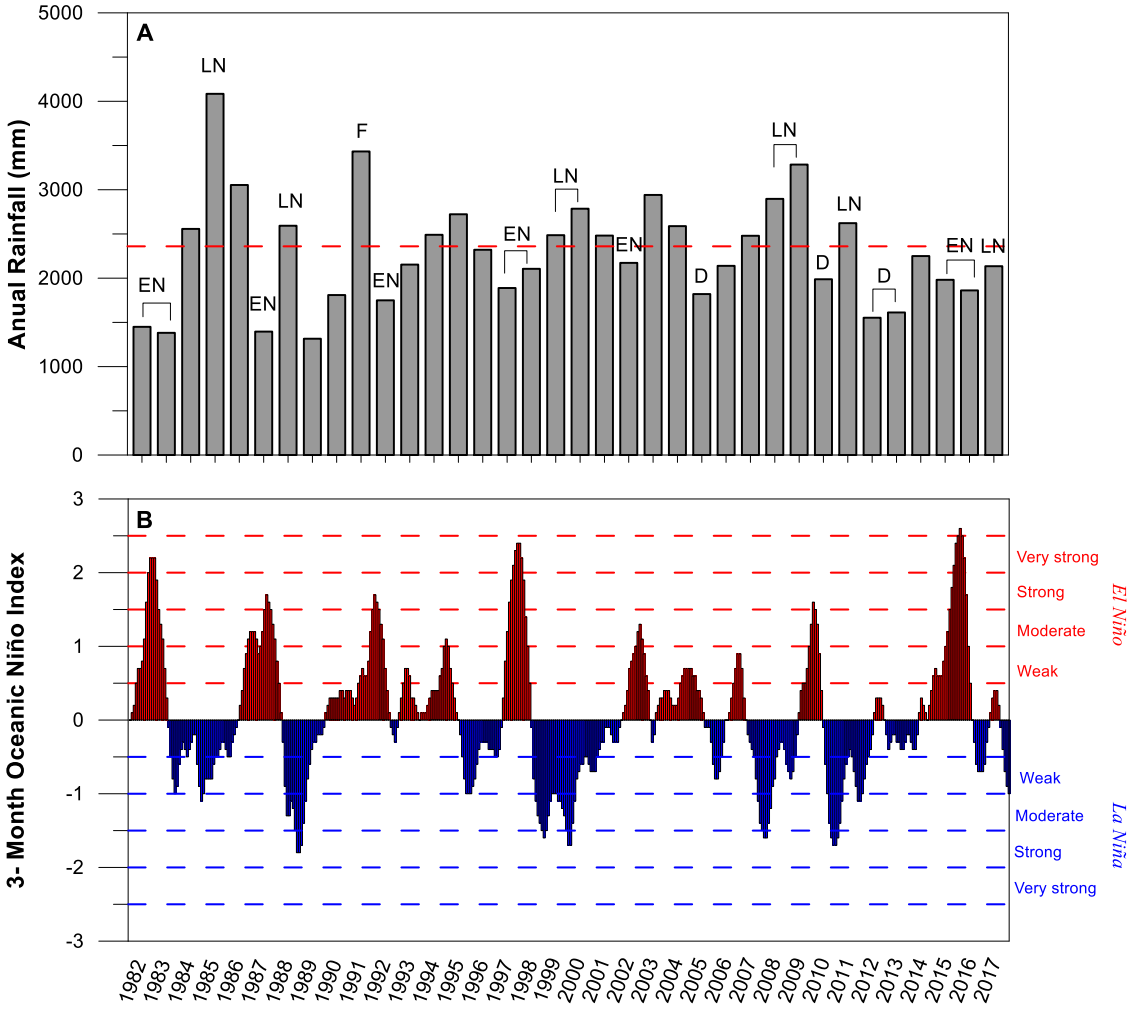

S1. (A) Total annual rainfall between 1982 and 2017 (source: INMET), highlighting the principal deviations in rainfall levels (LN = La Niña event; EN = El Niño event; F = Flood; D = Drought). Horizontal dashed line represents the historical mean annual rainfall level. (B) 3-Month Oceanic Niño Index, detaching El Niño and La Niña levels (source: NOAA).

Electronic Supplemental Material

Effects of extreme climatic events on the hydrological parameters of the estuarine waters of the Amazon Coast

Ádila Kelly Rodrigues da Costa[1], Luci Cajueiro Carneiro Pereira[1,*], José A. Jiménez[2], Antonio Rafael Gomes de Oliveira[1], Manuel de Jesus Flores-Montes[3] and Rauquírio Marinho da Costa[1]

[1]Universidade Federal do Pará, Instituto de Estudos Costeiros, Alameda Leandro Ribeiro sn, Aldeia, 68600-000, Braganca-Pará. [*]E-mail: cajueiro@ufpa.br.
[2]Universitat Politècnica de Catalunya - BarcelonaTech, Laboratori d'Enginyeria Marítima, C/Jordi Girona, 1-3, 08034, Barcelona, Spain.
[3]Universidade Federal de Pernambuco, Departamento de Oceanografia, Avenida Arquitetura, s/n, Cidade Universitária, Recife, Pernambuco.

S2. Data collection periods and rainfall condition.

Campaigns (Month/year)	Seasons	Climatic periods
Apr/12	Rainy	*Drought*[1]
Jun-12	Rainy	*Drought*[1]
Sep-12	Dry	*Drought*[1]
Dec/12	Dry	*Drought*[1]
Mar-13	Rainy	*Drought*[1]
Jun-13	Rainy	*Drought*[1]
Sep-13	Dry	*Drought*[1]
Nov-13	Dry	*Drought*[1]
Apr/14	Rainy	Typical[2]
Jun-14	Rainy	Typical[2]
Sep-14	Dry	Typical[2]
Dec/14	Dry	Typical[2]
Mar-15	Rainy	Typical[2]
Jun-15	Rainy	*El Niño*[3]
Sep-15	Dry	*El Niño*[3]
Dec/15	Dry	*El Niño*[3]
Apr/16	Rainy	*El Niño*[3]
Jun-16	Rainy	*El Niño*[3]
Sep-16	Dry	*El Niño*[3]
Nov-16	Dry	*El Niño*[3]
Apr/17	Rainy	*Typical*[2]

[1]Drought event: substantial dry conditions over Northern and Northeastern Brazil (Cunha et al., 2019).
[2]Typical condition: rainfall values similar to the historical means (INMET: 1982-2017).
[3]El Niño event: intense dry conditions over the Northeastern Amazon (Cunha et al., 2019).